Received: 5 February 2020 | Revised: 12 September 2020 | Accepted: 16 September 2020

DOI: 10.1002/ijfe.2296

RESEARCH ARTICLE

WILEY

A three-dimensional asymmetric power HEAVY model

Stavroula Yfanti[1] | **Georgios Chortareas**[2] | **Menelaos Karanasos**[3] | **Emmanouil Noikokyris**[4]

[1]School of Business and Economics, Loughborough University, Loughborough, UK

[2]King's Business School, King's College London, London, UK

[3]Department of Economics and Finance, Brunel University London, Uxbridge, UK

[4]School of Economics and Finance, Queen Mary University of London, London, UK

Correspondence
Stavroula Yfanti, School of Business and Economics, Loughborough University, Epinal Way, Loughborough LE11 3TU, UK.
Email: stavyfan@gmail.com

Abstract

This article proposes the three-dimensional HEAVY system of daily, intra-daily, and range-based volatility equations. We augment the bivariate model with a third volatility metric, the Garman–Klass estimator, and enrich the trivariate system with power transformations and asymmetries. Most importantly, we derive the theoretical properties of the multivariate asymmetric power model and explore its finite-sample performance through a simulation experiment on the size and power properties of the diagnostic tests employed. Our empirical application shows that all three power transformed conditional variances are found to be significantly affected by the powers of squared returns, realized measure, and range-based volatility as well. We demonstrate that the augmentation of the HEAVY framework with the range-based volatility estimator, leverage and power effects improves remarkably its forecasting accuracy. Finally, our results reveal interesting insights for investments, market risk measurement, and policymaking.

KEYWORDS

asymmetries, HEAVY model, high-frequency data, power transformations, realized volatility, risk management

JEL CLASSIFICATION

C22; C58; G01; G15

1 | INTRODUCTION

Financial volatility lies at the core of empirical finance research, with direct employment in investments, risk management practices, and financial stability oversight. Reliable modelling and accurate forecasting of the volatility pattern has been the main objective of financial applications for business operations, given that volatility is considered as one of the fundamental input variables in estimations and decision processes of any corporation on derivatives pricing, portfolio immunization, investment diversification, firm valuation, and funding choices. Financial volatility is also closely inspected by policymakers since it entails critical destabilizing threats for the financial system.

We develop a three-dimensional HEAVY[1] model by augmenting the bivariate system of Shephard and Sheppard (2010) with a third variable, namely, the range-based Garman–Klass volatility. Another contribution is the enrichment of the trivariate model with asymmetries and power transformations through the APARCH structure of Ding, Granger, and Engle (1993). Motivated by

the established merits of this framework, which considerably improves Bollerslev's (1986) GARCH process by adding leverage and power effects (see, for example, Brooks, Faff, McKenzie, & Mitchell, 2000, Karanasos & Kim, 2006), we similarly extend the trivariate system with these two features to explore its superiority over the benchmark specification. Most importantly, we derive the theoretical time series properties (optimal predictors and second moment structure) of the multivariate asymmetric power system and explore its finite-sample performance through a simulation experiment. We further proceed with an empirical application of the proposed model, to examine the various nested specifications in depth by investigating their performance over five stock indices. One of our key findings is that each of the three powered conditional variances is significantly affected by the first lags of all three power transformed variables, that is, squared negative returns, realized variance, and Garman–Klass volatility.

Following the burst of the 2008 crisis, when volatilities rose sharply and persistently with crucial systemic risk externalities, we witnessed a resurgence of regulators' and academics' interest in meaningful volatility estimates, while at the same time, practitioners remained alert to improving the relevant volatility frameworks on a day-to-day basis. Financial economics scholars focused on volatility as a potent catalyst of systemic risk build-up, which policymakers tried to limit. We demarcate this study from the extant finance bibliography by extending the benchmark HEAVY model with asymmetries, power transformations, and Garman–Klass volatility providing a well-defined framework that adequately fits the volatility process. We further examine the theoretical properties of the proposed model and demonstrate its forecasting superiority over the benchmark specification using a rolling window out-of-sample forecasting procedure. The three-dimensional system of volatility equations, we establish, is ready-to-use, not only on stock market returns but also on further asset classes or financial instruments (exchange rate, cryptocurrency, commodity, real estate, and bond returns) and multiple financial economics applications of business operations, such as bonds investing, foreign exchange trading and commodities hedging, core daily functions in the treasuries of most financial and non-financial corporations.

Overall, our proposed volatility modelling framework improves the HEAVY model, with important implications for market practitioners and policymakers on forecasting the trajectory of the financial returns' second moment. Volatility modelling and forecasting are essential for asset allocation, pricing, and risk hedging strategies. A reliable volatility forecast, exploiting in full the high-frequency domain, is the input variable of paramount importance for the processes of derivatives pricing, effective cross-hedging, Value-at-Risk (VaR) measurement, investment allocation, and portfolio optimization with different asset classes and financial instruments. Moreover, the robust volatility modelling approach we introduce provides a useful tool not only for market players but also for policymakers. Policymaking includes continuous oversight duties and prudential regulation practices. In this vein, it is imperative for the authorities to account for the volatility of financial markets across every aspect of the financial system's policy responses, both post-crisis through stabilization policy reactions and pre-crisis through proactive assessment of financial risks. The asymmetric power HEAVY framework we propose here has been shown to perform significantly better than the benchmark specification both in the short- and long-term forecasting horizons. Trading and risk management processes mostly use 1- to 10-day forecasts while policymakers are involved in longer-term predictions of financial volatility. Hence, we illustrate our model's forecasting superiority with a VaR example that provides both risk management and policy implications.

The remainder of the article is structured as follows. In Section 2, we detail the three-dimensional HEAVY formulation and our extension, which allows for asymmetries and power transformations. Section 3 introduces the theoretical properties of the multivariate asymmetric power HEAVY model and contains a simulation experiment on the finite-sample properties of the diagnostic tests employed. Section 4 describes the data and presents the results of the empirical application of the asymmetric power specification. In Section 5, we calculate multiple-step-ahead forecasts to measure the out-of-sample performance of the proposed specifications. Finally, Section 6 concludes the analysis.

2 | THE HEAVY FRAMEWORK

There are several studies introducing non-parametric estimators of realized volatility using high-frequency market data. Andersen and Bollerslev (1998), Andersen, Bollerslev, Diebold, and Labys (2001), and Barndorff-Nielsen and Shephard (2002) were the first that econometrically formalized the realized variance with quadratic variation-like measures, while Barndorff-Nielsen, Hansen, Lunde, and Shephard (2008, 2009) focused on the realized kernel estimation as a realized measure which is more robust to noise.

A large body of empirical research focuses on modelling and forecasting the realized volatility. Various studies combine it with the conditional variance of returns. Engle (2002b) proposed the GARCH-X process, where

the former is included as an exogenous variable in the equation of the latter. Corsi, Mittnik, Pigorsch, and Pigorsch (2008) suggested the HAR-GARCH formulation for modelling the volatility of realized volatility. Hansen, Huang, and Shek (2012) introduced the Realized GARCH model that corresponds more closely to the HEAVY framework of Shephard and Sheppard (2010), which jointly estimates conditional variances based on both daily (squared returns) and intra-daily (it uses the realized measure—kernel and variance—as a measure of ex-post volatility) data, so that the system of equations adopts to information arrival more rapidly than the classic daily GARCH process. One of its advantages is the robustness to certain forms of structural breaks, especially during the crisis periods, since the mean reversion and short-run momentum effects result in higher quality performance in volatility level shifts and more reliable forecasts. Borovkova and Mahakena (2015) employed a HEAVY specification with a skewed-t error distribution, while Huang, Liu, and Wang (2016) incorporated the HAR structure of the realized measure in the GARCH conditional variance specification in order to capture the long memory of the volatility dynamics.

The benchmark HEAVY model of Shephard and Sheppard (2010) can be extended in many directions. We allow for power transformations and leverage effects in the conditional variance process to improve volatility modelling and forecasting further (see also Data S1 on the enrichment of the trivariate asymmetric power specification with long memory features and structural breaks).

2.1 | Benchmark model

The HEAVY model uses two variables: the close-to-close stock returns (r_t) and the realized measure of variation based on high-frequency data, RM_t. We first form the signed square rooted (SSR) realized measure as follows: $R\tilde{M}_t = sign(r_t)\sqrt{RM_t}$, where $sign(r_t) = 1$, if $r_t \geqslant 0$ and $sign(r_t) = -1$, if $r_t < 0$.

In this article, we test the inclusion of an alternative measure of volatility to the HEAVY framework, that is we employ the classic range-based estimator of Garman and Klass (1980), hereafter GK. We further form the SSR GK volatility ($\tilde{GK}_t = sign(r_t)\sqrt{GK_t}$).

We assume that the returns, the SSR realized measure and GK volatility are characterized by the following relations:

$$r_t = e_{rt}\sigma_{rt}, R\tilde{M}_t = e_{Rt}\sigma_{Rt}, \tilde{GK}_t = e_{gt}\sigma_{gt}, \quad (1)$$

where the stochastic term e_{it} is independent and identically distributed (*i.i.d*), $i = r, R, g$; σ_{it} is positive with probability one for all t and it is a measurable function of $\mathcal{F}_{t-1}^{(XF)}$, that is the filtration generated by all available information through time $t-1$. We will use $\mathcal{F}_{t-1}^{(HF)}$ ($X = H$) for the high-frequency past data, that is, for the case of the realized measure, or $\mathcal{F}_{t-1}^{(LoF)}$ ($X = Lo$) for the low-frequency past data, that is, for the case of the close-to-close returns. Hereafter, for notational convenience, we will drop the superscript XF.

In the HEAVY/GARCH model e_{it} has zero mean and unit variance. Therefore, the three series have zero conditional means, and their conditional variances are given by:

$$\mathbb{E}\left(r_t^2|\mathcal{F}_{t-1}\right) = \sigma_{rt}^2, \mathbb{E}\left(R\tilde{M}_t{}^2|\mathcal{F}_{t-1}\right) = \mathbb{E}(RM_t|\mathcal{F}_{t-1}) = \sigma_{Rt}^2, \text{and} \mathbb{E}\left(\tilde{GK}_t^2|\mathcal{F}_{t-1}\right) = \mathbb{E}(GK_t|\mathcal{F}_{t-1}) = \sigma_{gt}^2, \quad (2)$$

where $\mathbb{E}(\cdot)$ denotes the expectation operator. The three equations are called HEAVY-i, $i = r, R, g$ for the returns, the realized measure, and Garman–Klass volatility, respectively.

2.2 | Asymmetric power formulation

The asymmetric power (AP) specification for the three-dimensional (3D) HEAVY(1, 1) consists of the following equations (in what follows for notational simplicity, we will drop the order of the model if it is (1, 1)):

$$\begin{aligned}(1-\beta_i L)\left(\sigma_{it}^2\right)^{\frac{\delta_i}{2}} = \omega_i &+ (\alpha_{ir} + \gamma_{ir}s_{t-1})L\left(r_t^2\right)^{\frac{\delta_r}{2}} \\ &+ (\alpha_{iR} + \gamma_{iR}s_{t-1})L(RM_t)^{\frac{\delta_R}{2}} \\ &+ \left(\alpha_{ig} + \gamma_{ig}s_{t-1}\right)L(GK_t)^{\frac{\delta_g}{2}},\end{aligned} \quad (3)$$

where L is the lag operator, $\delta_i \in \mathbb{R}_{>0}$ (the set of the positive real numbers) are the power parameters, for $i = r, R$, g, and $s_t = 0.5[1 - sign(r_t)]$, that is, $s_t = 1$ if $r_t < 0$ and 0 otherwise; γ_{ii}, γ_{ij} ($i \neq j$) are the own and cross leverage parameters, respectively[2]; positive γ_{ii}, γ_{ij} means larger contribution of negative 'shocks' in the volatility process (in our long memory AP specification we will replace $\alpha_{ii} + \gamma_{ii}s_{t-1}$ by $\alpha_{ii}(1 + \gamma_{ii}s_{t-1})$; see Data S1). In this specification the powered conditional variance, $\left(\sigma_{it}^2\right)^{\delta_i/2}$, is a linear function of the lagged values of the power transformed squared returns, realized measure and GK volatility.

We will distinguish between three different asymmetric cases: the double one (DA: $\gamma_{ij} \neq 0$ for all i and j) and two more, own asymmetry (OA: $\gamma_{ij} = 0$ for $i \neq j$ only) and cross asymmetry (CA: $\gamma_{ii} = 0$).

The α_{iR} and γ_{iR} are called the (six) Heavy parameters (own when $i = R$ and cross when $i \neq R$). These parameters capture the impact of the realized measure on the three conditional variances. Similarly, the α_{ir} and γ_{ir} (six in total) are called the Arch parameters (own when $i = r$ and cross for $i \neq r$). They depict the influence of the squared returns on the three conditional variances. Finally, the α_{ig} and γ_{ig} are called the (six) Garman parameters. These parameters capture the effects of the GK volatility on the three conditional variances.

The asymmetric power model is equivalent to a trivariate AP-GARCH process for the returns, the SSR realized measure, and GK volatility (see, for example, Conrad & Karanasos, 2010). If all 12 Arch and Garman parameters are zero, then we have the AP version of the benchmark HEAVY specification where the only unconditional regressor is the first lag of the powered RM_t. Finally, we should mention that all the parameters in this trivariate system should take non-negative values (see, for example, Conrad & Karanasos, 2010).

To sum up, the bivariate benchmark model (Equation (2)) of Shephard and Sheppard (2010)[3] is characterized by two conditional variance equations, the GARCH(1,0)-X formulation for returns and the GARCH (1,1) formulation for the SSR realized measure:

$$\text{HEAVY-}r: (1-\beta_r L)\sigma_{rt}^2 = \omega_r + \alpha_{rR} L(RM_t),$$
$$\text{HEAVY-}R: (1-\beta_R L)\sigma_{Rt}^2 = \omega_R + \alpha_{RR} L(RM_t).$$

Equation (3) gives the general formulation of our asymmetric power extension, which adds asymmetries, power transformations, and the GK volatility to the benchmark specification. We also use the existing Gaussian quasi-maximum likelihood estimators (QMLE) and multistep-ahead predictors already applied in the APARCH framework (see, for example, He & Teräsvirta, 1999; Karanasos & Kim, 2006; Laurent, 2004). We will first estimate the three conditional variance equations in the general form with all Heavy, Arch, Garman, and Asymmetry parameters given by Equation (3) and in case a parameter is insignificant, we will exclude it and this will result in a reduced form that is statistically preferred for each volatility process. Before the empirical illustration of the proposed model on stock index volatility, we first derive the time series properties of the multivariate AP-HEAVY system and examine its finite-sample performance through a simulation experiment.

3 | THEORETICAL PROPERTIES OF THE MULTIVARIATE AP-HEAVY MODEL

3.1 | Notation

Throughout this section, we adhere to the following conventions:

Notation 1 $(\mathbb{Z}_{>0})$ $\mathbb{Z}$, and $\mathbb{Z}_{\geq 0}$ stand for the sets of (positive) integers, and non-negative integers respectively. Similarly, $(\mathbb{R}_{>0})$ $\mathbb{R}$ and $\mathbb{R}_{\geq 0}$ stands for the set of (positive) real numbers, and non-negative real numbers respectively.

Notation 2 We will use upper (lower) case boldface symbols to refer to square matrices (vectors). That is, $\mathbf{y} = [y_i]_{i = 1,\ldots,N}$ is an $N \times 1$ column vector, $\mathbf{Y} = [y_{ij}]_{i,j = 1,\ldots,N}$ is a square matrix of order N.

$\mathbf{I}_N$ is the N-dimensional identity matrix (hereafter, we will drop the subscript for notational simplicity).

Notation 3 Using standard notation, $\mathbf{Y}'$ and $\mathbf{Y}^{-1}$ are the transpose and the inverse of the square matrix $\mathbf{Y}$. $\mathbf{Y}^{\wedge k} = \left[y_{ij}^k\right]$ is the element-wise exponentiation, whereas $\mathbf{y}^{\wedge \mathbf{x}} = [y_i^{x_i}]$, that is the element occupying the ith entry of vector $\mathbf{y}$ is raised to the power of the element occupying the ith entry of vector $\mathbf{x}$. $\mathbf{Y}^k = {}_{i=1}^{k}\mathbf{Y}$ means that the matrix $\mathbf{Y}$ is raised to the power of k.

In addition, $diag[\mathbf{y}]$, and $diag[\mathbf{Y}]$ denote diagonal matrices with elements y_i and y_{ii}, respectively.

We will refer to the element-wise absolute value of $\mathbf{Y}$ as $|\mathbf{Y}| = [|y_{ij}|]$. Finally, the inequality $\mathbf{Y} \geq \mathbf{0}$ means that all elements of $\mathbf{Y}$ are non-negative real numbers.

Notation 4 The element-wise expectation operator is denoted by $\mathbb{E}$, that is, $\mathbb{E}(\mathbf{Y}) = \left[\mathbb{E}\left(y_{ij}\right)\right]$ (similarly, $\mathbb{E}(\mathbf{Y}|\mathcal{F}_{t-1})$ denotes the element-wise, conditional on time $t-1$, expectation operator).

Notation 5 Let $\mathbf{Y}^{\otimes 2} = \mathbf{Y} \otimes \mathbf{Y}$, where $\otimes$ is the Kronecker product of two matrices, and $vec(\mathbf{Y})$ is a vector in which the columns of the matrix $\mathbf{Y}$ are stacked one underneath the other.

3.2 | Multivariate system

In this section, we will examine the theoretical properties of the multivariate AP-HEAVY model. We will consider the N-dimensional vector process, $\mathbf{r}_t = [r_{it}]$, $i = 1, \ldots, N$,

$N \in \mathbb{Z}_{\geq 1}$, $t \in \mathbb{Z}$. For example, for the trivariate case, $r_{1t} = r_t$, $r_{2t} = \tilde{RM}_t$, and $r_{3t} = \tilde{GK}_t$. Similarly to Equation (1), we assume that the vector $\mathbf{r}_t$ is characterized by the relation:

$$\mathbf{r}_t = \mathbf{Z}_t \sigma_t, \tag{4}$$

where $\mathbf{Z}_t = diag[\mathbf{e}_t]$, $\mathbf{e}_t = [e_{it}]$, and $\boldsymbol{\sigma}_t = [\sigma_{it}]$ is $\mathcal{F}_{t-1}$ measurable with $\mathcal{F}_{t-1} = \sigma(\mathbf{r}_{t-1}, \mathbf{r}_{t-2}, ...)$ with $\boldsymbol{\sigma}_t > \mathbf{0}$ for all t. That is, $\mathbf{r}_t = [e_{it}\sigma_{it}]$. Analogously with the assumptions in Section 2.1 the stochastic vector $\mathbf{e}_t = [e_{it}]$ is independent and identically distributed (i.i.d) with $\mathbb{E}\left(|e_{it}|^{\delta_i}|e_{jt}|^{\delta_j}\right) \in \mathbb{R}_{>0}$ for $i, j = 1, ..., N$.

In the N-dimensional (constant conditional correlation) multivariate GARCH model $\mathbf{e}_t$ has zero mean, unit variance, and positive definite time invariant conditional correlation matrix $\mathbf{R} = [\rho_{ij}]$ with $\rho_{ii} = 1$. The conditional covariance matrix of $\mathbf{r}_t$ is denoted by $\mathbf{H}_t = \mathbb{E}(\mathbf{r}_t\mathbf{r}_t'|\mathcal{F}_{t-1})$, and it is given by $\mathbf{H}_t = \Sigma_t \mathbf{R} \Sigma_t$, where $\Sigma_t = diag[\boldsymbol{\sigma}_t] = diag\left[\mathbf{H}_t^{\frac{1}{2}}\right]$.

The N-dimensional AP-HEAVY(1, 1) model is given by:

$$(\mathbf{I} - \mathbf{B}L)\boldsymbol{\sigma}_t^{\wedge\boldsymbol{\delta}} = \boldsymbol{\omega} + L\mathbf{A}_t|\mathbf{r}_t|^{\wedge\boldsymbol{\delta}}, \tag{5}$$

where $\boldsymbol{\delta} = [\delta_i]$, is the vector with the power parameters with $\delta_i \in \mathbb{R}_{>0}$ for all i, $\boldsymbol{\sigma}_t^{\wedge\boldsymbol{\delta}} = \left[\sigma_{it}^{\delta_i}\right]$, and $|\mathbf{r}_t|^{\wedge\boldsymbol{\delta}} = \left[|e_{it}|^{\delta_i}\sigma_{it}^{\delta_i}\right]$ (we recall that $\mathbf{r}_t$ and $\boldsymbol{\sigma}_t$ have been defined in Equation (4)). $\mathbf{B} = [\beta_{ii}]$ is a diagonal matrix (of order N); $\boldsymbol{\omega} = [\omega_i]$ is a vector that contains the drifts; $\mathbf{A}_t = \mathbf{A} + \Gamma_t$, where $\mathbf{A} = [\alpha_{ij}]$ and $\Gamma_t = \left[\gamma_{ij}s_{jt}\right]$, are N-dimensional full matrices. Note that Γ_t can be written as $\Gamma_t = \Gamma diag[\mathbf{s}_t]$ where $\Gamma = \left[\gamma_{ij}\right]$ and $\mathbf{s}_t = [s_{it}]$. The cross diagonal elements of $\mathbf{A}$ capture the shock (or unconditional) spillovers, whereas those of Γ_t capture the asymmetric shock spillovers.

3.2.1 | Weak VARMA representation

In order to derive the optimal predictors, we need to obtain the weak VARMA representation of the model in Equation (5). First, we will introduce the following definitions.

Definition 1 (i) Let $\mathbf{Z}(\boldsymbol{\delta}) = \mathbb{E}\left(|\mathbf{Z}_t|^{\wedge\boldsymbol{\delta}}\right)$ be a diagonal matrix with the element occupying the ith entry denoted by $z_i = \mathbb{E}\left(|e_{it}|^{\delta_i}\right)$,

(ii) Define the serially uncorrelated vector with, under (see below) Condition 1, zero mean as follows: $\mathbf{v}_t(\boldsymbol{\delta}) = |\mathbf{r}_t|^{\wedge\boldsymbol{\delta}} - \mathbb{E}\left(|\mathbf{r}_t|^{\wedge\boldsymbol{\delta}}|\mathcal{F}_{t-1}\right)$. In view of Equation (4), $\mathbf{v}_t$ can be written as:

$$\mathbf{v}_t = |\mathbf{r}_t|^{\wedge\boldsymbol{\delta}} - \mathbf{Z}\boldsymbol{\sigma}_t^{\wedge\boldsymbol{\delta}} = \left(|\mathbf{Z}_t|^{\wedge\boldsymbol{\delta}} - \mathbf{Z}\right)\sigma_t^{\wedge\boldsymbol{\delta}},$$

(to lighten the notation, in what follows we drop the parenthesis $\boldsymbol{\delta}$; we recall that $\boldsymbol{\delta}$ is given in Equation (5).

Proposition 1 *The weak VARMA (1,1) representation of the N-dimensional AP-HEAVY (1, 1) process is given by*:

$$[\mathbf{I} - L\mathbf{C}_t]\boldsymbol{\sigma}_t^{\wedge\boldsymbol{\delta}} = \boldsymbol{\omega} + L\mathbf{A}_t\mathbf{v}_t, \tag{6}$$

where,

$$\mathbf{C}_t = \mathbf{B} + \mathbf{A}_t\mathbf{Z},$$

($\mathbf{B}$ and $\mathbf{A}_t$ have been defined in Equation (5); notice that $\mathbf{C}_t$ depends on $\boldsymbol{\delta}$, but again in order to simplify the notation we will use $\mathbf{C}_t$ instead of $\mathbf{C}_t(\boldsymbol{\delta})$).

The proof is trivial: we add and subtract $\mathbf{A}_{t-1}\mathbf{Z}\boldsymbol{\sigma}_{t-1}^{\wedge\boldsymbol{\delta}}$ in the right-hand side of Equation (5).

Next, let us call:

$$\mathbf{D}_{t,k} = \prod_{r=0}^{k-1} \mathbf{C}_{t-1-r}, \tag{7}$$

where $k \in \mathbb{Z}_{\geq 1}$. We further extend the definition of $\mathbf{D}_{t,k}$ by assigning the initial matrix value $\mathbf{D}_{t,0} = \mathbf{I}_N$.

3.2.2 | General solution

Next, we will present the general solution, which generates all the main time series properties of the AP-HEAVY multivariate system.

Theorem 1 *The general solution of the weak VARMA representation in Equation (6) under the initial matrix value* $\boldsymbol{\sigma}_{t-k}^{\wedge\boldsymbol{\delta}}$, *is given by*:

$$\boldsymbol{\sigma}_t^{\wedge\boldsymbol{\delta}} = \underbrace{\sum_{r=1}^{k} \mathbf{D}_{t,r-1}(\boldsymbol{\omega} + \mathbf{A}_{t-r}\mathbf{v}_{t-r})}_{\text{(Particular Solution)}} + \underbrace{\mathbf{D}_{t,k}\boldsymbol{\sigma}_{t-k}^{\wedge\boldsymbol{\delta}}}_{\text{(Homogeneous Sol.)}}. \tag{8}$$

The proof is trivial. It is obtained by using repeated substitution in Equation (6).

In the above Proposition $\boldsymbol{\sigma}_t^{\wedge\boldsymbol{\delta}}$ is decomposed into two parts. The homogeneous solution, which consists of the initial (matrix) value $\boldsymbol{\sigma}_{t-k}^{\wedge\boldsymbol{\delta}}$ times $\mathbf{D}_{t,k}$, and the particular one that is formed by products involving the matrix $\mathbf{D}_{t,r-1}$ times (i) the drift $\boldsymbol{\omega}$, and (ii) the matrix $\mathbf{A}_{t-r}$ times the serially uncorrelated vector $\mathbf{v}_{t-r}$.

Remark 1 When $k = 1$ the general solution in Theorem 1 coincides with Equation (6). This is a consequence of the following statement: $\mathbf{D}_{t,0} = \mathbf{I}$ and $\mathbf{D}_{t,1} = \mathbf{C}_{t-1}$ (see Equation (7)).

3.2.3 | Optimal predictors

In what follows, we will obtain the linear predictor of the AP-HEAVY system.

First, we will introduce some additional notation.

Notation 6 (i) Let the expected value of $\mathbf{C}_t$ and $\mathbf{A}_t$ be denoted as $\mathbf{C} = \mathbb{E}(\mathbf{C}_t)$ and $\bar{\mathbf{A}} = \mathbb{E}(\mathbf{A}_t)$, respectively (where $\mathbf{C}_t$ is given in Equation (6)). Thus,

$$\mathbf{C} = \mathbf{B} + \bar{\mathbf{A}}\mathbf{Z}, with \bar{\mathbf{A}} = \left(\mathbf{A} + \Gamma\frac{\mathbf{1}}{\mathbf{2}}\right), \tag{9}$$

(since $\mathbb{E}[diag\,\mathbf{s}_t]] = \mathbb{E}\left[diag\,\mathbf{s}_t^2\right]] = (1/2)\mathbf{I}$), and thus Equation (7) implies that $\mathbb{E}(\mathbf{D}_{t,k}) = \mathbf{C}^k$.

(ii) Let $\rho_{\max}(\mathbf{C})$ refer to the modulus of the largest eigenvalue of $\mathbf{C}$.

(iii) Let (Ω, F, P) be a probability space and $L_2(\Omega, F, P)$ (in short L_2) be the Hilbert space of random variables with finite first and second moments defined on (Ω, F, P).

Condition 1 $\rho_{\max}(\mathbf{C}) < 1$.

Taking the conditional expectation of Equation (8) with respect to the σ field $\mathcal{F}_{t-k-1}$ yields the following Proposition.

Proposition 2 *The k-step-ahead optimal (in L_2 sense) linear predictor of the powered transformed $\boldsymbol{\sigma}_t$ for the N-dimensional AP-HEAVY(1, 1) model is readily seen to be*:

$$\mathbb{E}\left(\boldsymbol{\sigma}_t^{\wedge\boldsymbol{\delta}}|\mathcal{F}_{t-k-1}\right) = (\mathbf{I}-\mathbf{C})^{-1}\left(\mathbf{I}-\mathbf{C}^k\right)\boldsymbol{\omega} + \mathbf{C}^k\boldsymbol{\sigma}_{t-k}^{\wedge\boldsymbol{\delta}}. \tag{10}$$

Under Condition 1 the unconditional mean of $\boldsymbol{\sigma}_t^{\wedge\boldsymbol{\delta}}$, that is $\boldsymbol{\sigma}(\delta) = \mathbb{E}\left(\boldsymbol{\sigma}_t^{\wedge\delta}\right)$ is equal to the $\lim_{k\to\infty}\mathbb{E}\left(\boldsymbol{\sigma}_t^{\wedge\boldsymbol{\delta}}|\mathcal{F}_{t-k-1}\right)$, and thus it is given by:

$$\boldsymbol{\sigma} = (\mathbf{I}-\mathbf{C})^{-1}\boldsymbol{\omega}. \tag{11}$$

(where $\mathbf{C}$ has been defined in Equation (9)).

Finally, the following Proposition gives the optimal linear predictor of the power transformed observed vector $|\mathbf{r}_t|^{\wedge\boldsymbol{\delta}}$ as well as its first unconditional moment.

Proposition 3 *The k-step-ahead optimal (in L_2 sense) linear predictor of $|\mathbf{r}_t|^{\wedge\boldsymbol{\delta}}$ is given by*:

$$\mathbb{E}\left(|\mathbf{r}_t|^{\wedge\boldsymbol{\delta}}|\mathcal{F}_{t-k-1}\right) = \mathbf{Z}\mathbb{E}\left(\boldsymbol{\sigma}_t^{\wedge\boldsymbol{\delta}}|\mathcal{F}_{t-k-1}\right),$$

($\mathbf{Z}$ has been defined in Definition 1(i), and Equation (10) gives $\mathbb{E}\left(\boldsymbol{\sigma}_t^{\wedge\boldsymbol{\delta}}|\mathcal{F}_{t-k-1}\right)$).

Under Condition 1, the unconditional mean of $|\mathbf{r}_t|^{\wedge\boldsymbol{\delta}}$, that is $\mathbf{r}(\boldsymbol{\delta}) = \mathbb{E}\left(|\mathbf{r}_t|^{\wedge\boldsymbol{\delta}}\right)$ is equal to $\lim_{k\to\infty}\mathbb{E}\left(|\mathbf{r}_t|^{\wedge\boldsymbol{\delta}}|\mathcal{F}_{t-k-1}\right)$, and thus it is given by:

$$\mathbf{r} = \mathbf{Z}\boldsymbol{\sigma}. \tag{12}$$

The proof is trivial. It follows from the definition of $|\mathbf{r}_t|^{\wedge\boldsymbol{\delta}}$ in Equation (4) and Proposition 2. Alternatively, we could obtain the optimal linear predictor and the first unconditional moment of $|\mathbf{r}_t|^{\wedge\boldsymbol{\delta}}$ using its weak VARMA(1, 1) representation, which is not difficult to show (proof is not reported but it is available upon request) that it is given by:

$$\mathbf{I} - L\mathbf{C}_t]|\mathbf{r}_t|^{\wedge\boldsymbol{\delta}} = \mathbf{Z}\boldsymbol{\omega} + (\mathbf{I}-\mathbf{B}L)\mathbf{v}_t.$$

A comparison

Next, we provide a comparison between the benchmark HEAVY system and the more general AP specification. Their difference is captured by the matrix $\mathbf{C}$ (see Equation (9)). We will examine the bivariate case, which is when $N = 2$. For the more general double asymmetric power (DAP) specification, $\mathbf{C}$ is a full matrix with: (i) diagonal elements given by $\beta_i + (\alpha_{ii} + \gamma_{ii}/2)z_i$, $i = r, R$, we recall that $z_i = \mathbb{E}\left(|e_{it}|^{\delta_i}\right)$, and (ii) off-diagonal elements given by $(\alpha_{ij} + \gamma_{ij})z_j$, $i, j = r, R$, for $i \neq j$. For the benchmark model, since $\gamma_{ij} = 0$, $z_i = 1$, for all $i, j = r, R$, and $\alpha_{Ri} = 0$, $\mathbf{C}$ is restricted to being an upper diagonal matrix. That is, we have:

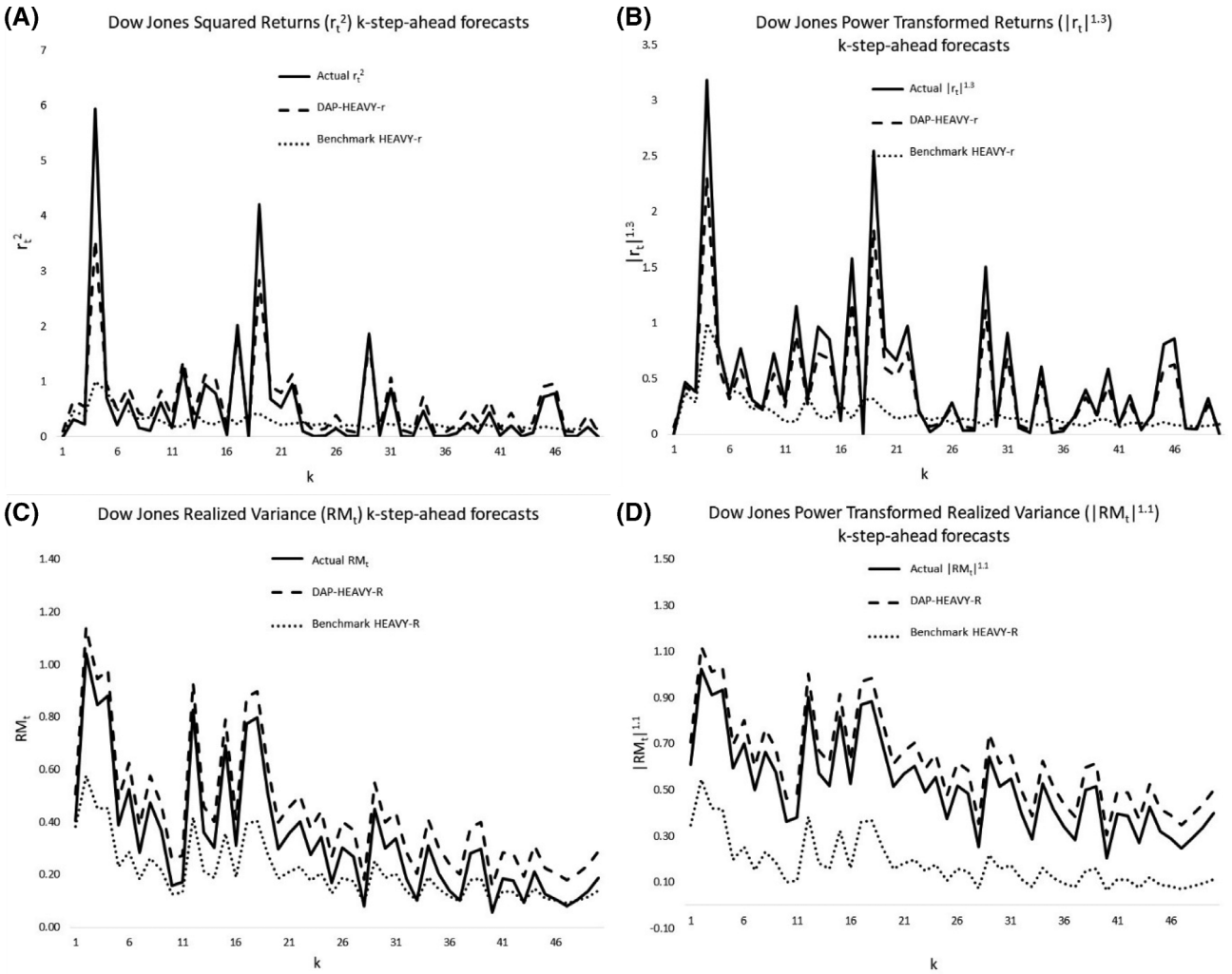

FIGURE 1 Dow Jones returns and realized variance *k*-step-ahead forecasts

DAP Specification :

$$\mathbf{C} = \begin{bmatrix} \beta_r + (\alpha_{rr} + \gamma_{rr}/2)z_r & (\alpha_{rR} + \gamma_{rR}/2)z_R \\ (\alpha_{Rr} + \gamma_{Rr}/2)z_r & \beta_R + (\alpha_{RR} + \gamma_{RR}/2)z_R \end{bmatrix}$$

Benchmark HEAVY : $\mathbf{C} = \begin{bmatrix} \beta_r & \alpha_{rR} \\ 0 & \beta_R + \alpha_{RR} \end{bmatrix}$.

Figure 1 presents the comparison of the benchmark and DAP-HEAVY models' forecasting performance (see also Section 5). We apply the optimal predictor of $|\mathbf{r}_t|^{\wedge\boldsymbol{\delta}}$ (under Proposition 3) on Dow Jones returns and realized variance data and calculate 50-step-ahead forecasts. The more general specification produces forecasts significantly closer to the actual values for both returns (Figure 1a,b) and realized measure (Figure 1c,d). Most importantly, its forecasts are more accurate in peaks of returns and realized variance actual values. The benchmark model remains behind our proposed asymmetric power extension in predicting low- and high-frequency volatility indicators. It produces, mostly, lower volatility forecasts (dotted lines) in comparison with the DAP (dashed lines) and actual (solid lines) values. Therefore, our first contribution, which is the asymmetric power extension, provides a significant improvement on the HEAVY system of Shephard and Sheppard (2010).

3.3 | Second moments

Now that we have derived the optimal predictors and the first unconditional moment of the AP-HEAVY system, we will examine its second moment structure.

3.3.1 | Notation

But first, we will introduce some further notation.

Covariances

Let $\Gamma(\ell;\boldsymbol{\delta}) = \left[\gamma_{ij}(\ell;\boldsymbol{\delta})\right]$, $\ell \in \mathbb{Z}_{\geq 0}$, be the multidimensional covariance function of $\left\{\boldsymbol{\sigma}_t^{\wedge\boldsymbol{\delta}}\right\}$; as usual in what follows

we will suppress the index $\boldsymbol{\delta}$ for ease of notation, that is we will use $\Gamma(\ell;\boldsymbol{\delta})=\Gamma(\ell)$. In view of this definition we have:

$$\Gamma(\ell)=\mathbb{E}\left[\left(\boldsymbol{\sigma}_{t-\ell}^{\wedge\boldsymbol{\delta}}-\sigma\right)\left(\boldsymbol{\sigma}_{t}^{\wedge\boldsymbol{\delta}}-\boldsymbol{\sigma}\right)'\right]=\Sigma(\ell)-\boldsymbol{\sigma}\boldsymbol{\sigma}', \tag{13}$$

where $\Sigma(\ell)=\mathbb{E}\left(\boldsymbol{\sigma}_{t-\ell}^{\wedge\boldsymbol{\delta}}\left(\boldsymbol{\sigma}_{t}^{\wedge\boldsymbol{\delta}}\right)'\right)$. In addition, let the vectorizations of $\Sigma(\ell)$ and $\Gamma(\ell)$ be denoted by $\mathbf{s}(\ell)$ and $\gamma(\ell)$, respectively. Explicit solutions for the $\Gamma(\ell)$ and conditions for its existence will be presented below.

Further, let

$$\mathbf{D}=diag\left[\sqrt{\gamma_{11}(0)},...,\sqrt{\gamma_{NN}(0)}\right],$$

where $\gamma_{ii}(0)$ is the element occupying the ith diagonal entry of $\Gamma(0)$. To further fix notation, write the ℓ-th order, for $\ell\geq 1$, autocorrelation matrix of $\boldsymbol{\sigma}_{t}^{\wedge\boldsymbol{\delta}}$ as:

$$\mathbf{R}(\ell)=\mathbf{D}^{-1}\Gamma(\ell)\mathbf{D}^{-1}.$$

Kronecker products

In what follows we will introduce some additional notation, which involves various Kronecker products.

Notation 7 Let

$$\mathbf{C}^{\otimes 2}=\mathbf{C}\otimes\mathbf{C},\quad \bar{\mathbf{A}}^{\otimes 2}=\bar{\mathbf{A}}\otimes\bar{\mathbf{A}}, \tag{14}$$

where $\mathbf{C}$ and $\bar{\mathbf{A}}$ have been defined in Equation (9).

We continue by introducing the following notation.

Notation 8 Let

$$\mathbf{Z}^{\otimes 2}=\mathbf{Z}\otimes\mathbf{Z},\mathbb{E}\left[\left(|\mathbf{Z}_t|^{\wedge\boldsymbol{\delta}}\right)^{\otimes 2}\right]=\mathbb{E}\left(|\mathbf{Z}_t|^{\wedge\boldsymbol{\delta}}\otimes|\mathbf{Z}_t|^{\wedge\boldsymbol{\delta}}\right),$$
$$\tilde{\mathbf{Z}}=\left[\mathbb{E}\left(|\mathbf{Z}_t|^{\wedge\boldsymbol{\delta}}\right)^{\otimes 2}\right]-\mathbf{Z}^{\otimes 2}=\mathbb{E}\left[\left(|\mathbf{Z}_t|^{\wedge\boldsymbol{\delta}}-\mathbf{Z}\right)^{\otimes 2}\right],$$

be three diagonal matrices of order N^2 ($\mathbf{Z}_t$ and $\mathbf{Z}$ have been defined in Equation (4) and Definition 1(i), respectively).

Remark 2 The element occupying the rth diagonal entry of $\tilde{\mathbf{Z}}$, with $r=[(i-1)N+j]$, where $i, j = 1, ..., N$, is given by:

$$\mathbb{E}\left(|e_{it}|^{\delta_i}|e_{jt}|^{\delta_j}\right)-\mathbb{E}\left(|e_{(it}|^{\delta_i}\right)\mathbb{E}\left(|e_{jt}|^{\delta_j}\right).$$

Notation 9 Let

$$\tilde{\mathbf{C}}=\mathbf{C}^{\otimes 2}+\bar{\mathbf{A}}^{\otimes 2}\tilde{\mathbf{Z}}, \tag{15}$$

(where $\mathbf{C}^{\otimes 2}$ and $\bar{\mathbf{A}}^{\otimes 2}$ are given in Equation (14), and $\tilde{\mathbf{Z}}$ is defined in Notation 8.

Condition 2 $\rho_{\max}\left(\tilde{\mathbf{C}}\right)<1$..

3.3.2 | Covariance structure

In the following theorem, we will present an explicit formula for $\boldsymbol{\gamma}(0)$.

Theorem 2 *Consider the N-dimensional vector AP-HEAVY (1, 1) process. Under Condition 2 the vectorization of $\Gamma(0)$, is given by*:

$$\gamma(0)=\left(\mathbf{I}_{N^2}-\tilde{\mathbf{C}}\right)^{-1}\bar{\mathbf{A}}^{\otimes 2}\tilde{\mathbf{Z}}\boldsymbol{\sigma}^{\otimes 2}. \tag{16}$$

Further, $\boldsymbol{\gamma}(\ell)$, for $\ell\geq 1$, is given by:

$$\boldsymbol{\gamma}(\ell)=\left(\mathbf{C}^{\ell}\otimes\mathbf{I}\right)\boldsymbol{\gamma}(0). \tag{17}$$

Next, let us denote the multidimensional covariance function of $\{|\mathbf{r}_t|^{\wedge\boldsymbol{\delta}}\}$ by $\Gamma_r(\ell)=\left[\gamma_{ij,r}(\ell)\right]$.

Theorem 3 *Consider the N-dimensional vector AP-HEAVY (1, 1) process. Under Condition 2 the vectorization of $\Gamma_r(0)$, is given by*:

$$\boldsymbol{\gamma}_r(0)=\left[\mathbb{E}\left[\left(|\mathbf{Z}_t|^{\wedge\boldsymbol{\delta}}\right)^{\otimes 2}\right]\left(\mathbf{I}_{N^2}-\tilde{\mathbf{C}}\right)^{-1}\bar{\mathbf{A}}^{\otimes 2}+\mathbf{I}_{N^2}\right]\tilde{\mathbf{Z}}\boldsymbol{\sigma}^{\otimes 2}. \tag{18}$$

Moreover, $\boldsymbol{\gamma}_r(\ell)$, for $\ell\geq 1$, is given by:

$$\boldsymbol{\gamma}_r(\ell)=\mathbf{Z}\boldsymbol{\gamma}_r(0). \tag{19}$$

In Appendix A, we derive the proofs of Theorems 2 and 3.

3.4 | Simulations

After deriving the time series properties of the multivariate AP-HEAVY system, we examine the finite-sample

TABLE 1 DGPs for size and power simulations

Heavy models	DGPs	A	B	Γ	δ
Panel A: Size simulations					
Benchmark	DGP 1	$\begin{bmatrix} 0 & 0.30 \\ 0 & 0.40 \end{bmatrix}$	$\begin{bmatrix} 0.65 & 0 \\ 0 & 0.55 \end{bmatrix}$	$\begin{bmatrix} 0 & 0 \\ 0 & 0 \end{bmatrix}$	$\begin{bmatrix} 2.0 \\ 2.0 \end{bmatrix}$
Benchmark	DGP 2	$\begin{bmatrix} 0 & 0.20 \\ 0 & 0.40 \end{bmatrix}$	$\begin{bmatrix} 0.75 & 0 \\ 0 & 0.60 \end{bmatrix}$	$\begin{bmatrix} 0 & 0 \\ 0 & 0 \end{bmatrix}$	$\begin{bmatrix} 2.0 \\ 2.0 \end{bmatrix}$
Benchmark	DGP 3	$\begin{bmatrix} 0 & 0.25 \\ 0 & 0.35 \end{bmatrix}$	$\begin{bmatrix} 0.85 & 0 \\ 0 & 0.65 \end{bmatrix}$	$\begin{bmatrix} 0 & 0 \\ 0 & 0 \end{bmatrix}$	$\begin{bmatrix} 2.0 \\ 2.0 \end{bmatrix}$
Benchmark	DGP 4	$\begin{bmatrix} 0 & 0.18 \\ 0 & 0.25 \end{bmatrix}$	$\begin{bmatrix} 0.80 & 0 \\ 0 & 0.70 \end{bmatrix}$	$\begin{bmatrix} 0 & 0 \\ 0 & 0 \end{bmatrix}$	$\begin{bmatrix} 2.0 \\ 2.0 \end{bmatrix}$
Benchmark	DGP 5	$\begin{bmatrix} 0 & 0.30 \\ 0 & 0.30 \end{bmatrix}$	$\begin{bmatrix} 0.80 & 0 \\ 0 & 0.70 \end{bmatrix}$	$\begin{bmatrix} 0 & 0 \\ 0 & 0 \end{bmatrix}$	$\begin{bmatrix} 2.0 \\ 2.0 \end{bmatrix}$
Panel B: Power simulations					
OAP	DGP 6	$\begin{bmatrix} 0 & 0.10 \\ 0.05 & 0.10 \end{bmatrix}$	$\begin{bmatrix} 0.80 & 0 \\ 0 & 0.70 \end{bmatrix}$	$\begin{bmatrix} 0.08 & 0 \\ 0 & 0.10 \end{bmatrix}$	$\begin{bmatrix} 1.5 \\ 1.5 \end{bmatrix}$
CAP	DGP 7	$\begin{bmatrix} 0 & 0.10 \\ 0.05 & 0.10 \end{bmatrix}$	$\begin{bmatrix} 0.80 & 0 \\ 0 & 0.70 \end{bmatrix}$	$\begin{bmatrix} 0 & 0.08 \\ 0.10 & 0 \end{bmatrix}$	$\begin{bmatrix} 1.5 \\ 1.5 \end{bmatrix}$
DAP	DGP 8	$\begin{bmatrix} 0 & 0.10 \\ 0.05 & 0.10 \end{bmatrix}$	$\begin{bmatrix} 0.80 & 0 \\ 0 & 0.70 \end{bmatrix}$	$\begin{bmatrix} 0.08 & 0.10 \\ 0.05 & 0.10 \end{bmatrix}$	$\begin{bmatrix} 1.5 \\ 1.5 \end{bmatrix}$
DAP	DGP 9	$\begin{bmatrix} 0.04 & 0.10 \\ 0.05 & 0.10 \end{bmatrix}$	$\begin{bmatrix} 0.80 & 0 \\ 0 & 0.70 \end{bmatrix}$	$\begin{bmatrix} 0.05 & 0.05 \\ 0.05 & 0.10 \end{bmatrix}$	$\begin{bmatrix} 1.5 \\ 1.5 \end{bmatrix}$
DAP	DGP 10	$\begin{bmatrix} 0.04 & 0.10 \\ 0.05 & 0.10 \end{bmatrix}$	$\begin{bmatrix} 0.80 & 0 \\ 0 & 0.70 \end{bmatrix}$	$\begin{bmatrix} 0.05 & 0.05 \\ 0.05 & 0.10 \end{bmatrix}$	$\begin{bmatrix} 1.5 \\ 1.0 \end{bmatrix}$

Note: For all DGPs $\boldsymbol{\omega} = \begin{bmatrix} 0.01 \\ 0.02 \end{bmatrix}$.
Abbreviation: DGP, data-generating process.

performance of the diagnostic tests employed in terms of both their size and power properties. Given that simulation studies have already widely explored the finite-sample properties of the univariate (AP-)GARCH-X and the multivariate GARCH with volatility spillovers (**A** and **B** full matrices) but without asymmetries, that is the Γ full matrix, (see, for example, Francq & Thieu, 2019; Halunga & Orme, 2009; Li, Zhang, & Zhang, 2019; Lundbergh & Teräsvirta, 2002; Nakatani & Teräsvirta, 2009; Pedersen, 2017; Pedersen & Rahbek, 2019), here in the multivariate AP-HEAVY/GARCH case, we choose to focus our simulation experiment on the significance of the asymmetric effects, the sign bias test (SBT) of Engle and Ng (1993) accounting for both own and cross leverage of each equation in the system, and the likelihood-ratio test (LRT) for model selection (benchmark vs. AP-HEAVY). We conduct the Monte Carlo simulations in OxMetrics 7 for the bivariate case of the asymmetric Power specification with own and cross Arch and Heavy parameters. For each data-generating process (DGP) with Gaussian innovations drawn from the standard Normal distribution (e_{1t}, $e_{2t} \sim IIDN(0, 1)$), we use the sample sizes $T = 1,000$, 2,500, 5,000, 10,000 after discarding the first 1,000 observations to avoid initialization effects. All simulations are based on 5,000 replications and the empirical rejection frequencies are compared with the 5% nominal size of each test.

We first consider the size properties of the SBT statistic for the DGPs 1–5 reported in Table 1, Panel A. We test five different specifications of the bivariate benchmark Heavy. The SBT statistic is calculated on each equation (e_{1t} and e_{2t} processes) with similar results and the actual rejection frequencies from both equations are stated in Table 2, Panel A. The SBT results suggest that significant sign effects are omitted by the benchmark specification. For DGPs 3 and 5, the test is relatively undersized in the sample size $T = 1,000$ and slightly oversized in the sample size $T = 10,000$. Overall, our Monte Carlo experiment shows that in most cases the sign bias test has reasonable size properties quite close to the 5% nominal level in larger samples.

Next, the simulations for the power of the sign bias test are based on DGPs 6–10 (Table 1, Panel B)

TABLE 2 Size and power simulation results

	First equation (e_{1t})					Second equation (e_{2t})				
Panel A: Size simulations (SBT empirical rejection frequencies)										
T	DGP 1	DGP 2	DGP 3	DGP 4	DGP 5	DGP 1	DGP 2	DGP 3	DGP 4	DGP 5
1, 000	0.031	0.046	0.009	0.059	0.010	0.026	0.039	0.001	0.051	0.012
2, 500	0.035	0.041	0.030	0.044	0.045	0.031	0.040	0.036	0.040	0.047
5, 000	0.040	0.049	0.041	0.039	0.049	0.049	0.055	0.049	0.047	0.043
10,000	0.046	0.052	0.058	0.045	0.059	0.046	0.052	0.055	0.048	0.061
Panel B: Power simulations (SBT empirical rejection frequencies)										
T	DGP 6	DGP 7	DGP 8	DGP 9	DGP 10	DGP 6	DGP 7	DGP 8	DGP 9	DGP 10
1, 000	0.442	0.204	0.632	0.841	0.809	0.506	0.233	0.701	0.892	0.831
2, 500	0.261	0.356	0.891	0.992	0.878	0.286	0.447	0.856	0.976	0.924
5, 000	0.755	0.694	0.949	0.997	1.000	0.623	0.688	0.991	0.999	1.000
10,000	0.893	0.905	0.995	1.000	1.000	0.850	0.969	1.000	1.000	1.000
Panel C: LRT p-values for AP (unrestricted) versus benchmark (restricted) heavy specification										
T	DGP 6	DGP 7	DGP 8	DGP 9	DGP 10	DGP 6	DGP 7	DGP 8	DGP 9	DGP 10
1, 000	.043	.067	.011	.014	.000	.038	.044	.009	.020	.010
2, 500	.037	.055	.025	.018	.001	.042	.041	.019	.027	.003
5, 000	.049	.048	.008	.022	.031	.047	.051	.012	.026	.036
10,000	.050	.046	.030	.020	.018	.052	.048	.036	.018	.024

Note: Empirical rejection frequencies based on the 5% nominal level.
Abbreviations: AP, asymmetric power; DGP, data-generating process; LRT, likelihood-ratio test; SBT, sign bias test.

corresponding to five bivariate AP-HEAVY models. The **B** matrix remains diagonal as in the benchmark case, that is without volatility spillovers from the cross Garch effects ($\beta_{12} = \beta_{21} = 0$). The **A** matrix is either a full matrix with all own and cross Arch effects (DGPs 9 and 10) or with the own Arch effect excluded in the first equation (DGPs 6–8), similarly to the returns and the Garman–Klass volatility equations estimated in our empirical application (see Table 5, Panels A and C). The Γ matrix contains the leverage parameters, either own asymmetries (OAP model, DGP 6) or cross asymmetries (CAP model, DGP 7) or a full matrix with both own and cross asymmetric effects (DAP model, DGPs 8–10). The power transformations in $\boldsymbol{\delta}$ are common for both equations in the system with $\delta_i = 1.5$ for DGPs 6–9. In the case of DGP 10, we test different powers ($\delta_1 = 1.5$ and $\delta_2 = 1.0$) for the conditional variance of the two processes. Table 2, Panel B reports the SBT power simulation results with significant asymmetric effects not ignored across all AP-HEAVY models considered. The power of the test improves as the sample size increases for most DGPs, while in the DAP models with full Γ matrix (DGPs 8–10) the power is already high from smaller samples.

Finally, we perform the likelihood-ratio test of the AP model compared with the benchmark one for both equations. We consider DGPs 6–10 as the unrestricted specifications and the corresponding benchmark ones (with $\Gamma = \mathbf{0}$ and $\alpha_{11} = \alpha_{21} = 0$) as the restricted cases. The LRT results in Table 2, Panel C support the superiority of the asymmetric models to the benchmark formulations. The test suggests the significant improvement in terms of the log-likelihood maximization for the more richly parametrized unrestricted models versus the respective restricted cases.

All in all, the simulation experiment suggests very good size and power properties of the SBT in detecting asymmetries in the HEAVY framework and quite good performance of the LRT for model selection across all sample sizes. Furthermore, our simulation results have also shown that the empirical distribution of the t-statistics of all estimated parameters in both equations is quite close to normal (the average difference of the true parameter and its estimate [bias], the standard error and the root mean square error of the estimate are available upon request for all parameters), mostly converging to normal in higher sample sizes regardless of the degree of persistence tested under each DGP, and at the same time validating the finite-sample performance of the QML estimators. In the remaining part of the article, the AP-HEAVY model's overperformance in- and out-of-sample is further illustrated through an empirical application on stock index data (Sections 4 and 5).

4 | EMPIRICAL APPLICATION

4.1 | Data description

We provide an empirical application of the HEAVY framework on five stock indices' returns, realized and GK volatilities. We use daily data for five stock market indices extracted from the Oxford-Man Institute's (OMI) realized library version 0.3 of Heber, Lunde, Shephard, and Sheppard (2009): Dow Jones Industrial Average from the US (DJ), Korea Composite Stock Price Index from South Korea (KOSPI), CAC 40 from France (CAC), All Ordinaries from Australia (AORD), and MXSE IPC from Mexico (IPC). Our sample covers the period from 3 January 2000 to 30 September 2019 for most indices. The OMI's realized library includes daily stock market returns and several realized volatility measures calculated on high-frequency data from the Reuters DataScope Tick History database. The data are first cleaned and then used in the realized measures calculations. According to the library's documentation, the data cleaning consists of deleting records outside the time interval that the stock exchange is open. Some minor manual changes are also needed when results are ineligible due to the rebasing of indices. We use the daily closing prices, P_t^C, to form the daily returns as follows: $r_t = \ln(P_t^C) - \ln(P_{t-1}^C)$, and two realized measures as drawn from the library: the realized kernel and the 5-min realized variance. The estimation results using the two alternative measures are very similar, so we present only the ones with the realized variance (the results for the realized kernel are available upon request).

4.1.1 | Realized measures

The library's realized measures are calculated in the way described in Shephard and Sheppard (2010). The realized kernel, which we use as an alternative to the realized variance (results are not reported but they are available upon request), is calculated using a Parzen weight function as follows: $RK_t = \sum_{k=-H}^{H} k(h/(H+1))\gamma_h$, where $k(x)$ is the Parzen kernel function with $\gamma_h = \sum_{j=|h|+1}^{n} x_{j,t}x_{j-|h|,t}$; $x_{jt} = X_{t_{j,t}} - X_{t_{j-1,t}}$ are the 5-min intra-daily returns where $X_{t_{j,t}}$ are the intra-daily log-prices and $t_{j,t}$ are the times of trades on the tth day. Shephard and Sheppard (2010) declared that they selected the bandwidth of H as in Barndorff-Nielsen et al. (2009).

The 5-min realized variance, RV_t, which we choose to present here, is calculated with the formula: $RV_t = \sum x_{j,t}^2$. Heber et al. (2009) additionally implement a subsampling procedure from the data to the most feasible level in order to eliminate the stock market noise effects. The subsampling involves averaging across many realized variance estimations from different data subsets (see also the references in Shephard & Sheppard, 2010 for realized measures surveys', noise effects, and subsampling procedures).

4.1.2 | GK volatility

Using data on the daily high, low, opening, and closing prices of each index in the OMI's realized library we generate an additional daily measure of price volatility. To avoid the microstructure biases introduced by high-frequency data and based on the conclusion of Chen, Daigler, and Parhizgari (2006), that the range-based and high-frequency integrated volatility provide essentially equivalent results, we construct the daily GK volatility as follows:

$$GK_t = \frac{1}{2}u_t^2 - (2\ln 2 - 1)c_t^2,$$

where u_t and c_t are the differences in the natural logarithms (as of time t) of the high and low and of the closing and opening prices, respectively. The Garman–Klass is an open-to-close range-based volatility estimator that is documented as a more precise volatility proxy, with superior empirical performance in the GARCH framework. Recently, Molnár (2016) has demonstrated that the inclusion of the Parkinson and GK estimators in the Range-GARCH model he proposed, outperforms the standard GARCH(1, 1), and it performs particularly better in situations, where volatility level changes rapidly. Several studies have also discussed the improvement of the GARCH framework through the open-to-close range-based volatility proxies, regarded as more accurate than the close-to-close squared returns: they exclude the noise from the dynamics of the opening jumps and they ensure greater accuracy in volatility forecasting through the range information they provide (see Chou, Chou, & Liu, 2010, 2015; Molnár, 2012 and the references therein). Therefore, we incorporate the GK variable in our HEAVY system, in order to improve the model's forecasting performance.

Table 3 presents the five stock indices extracted from the database and provides volatility estimations for each one's squared returns, realized variances, and GK volatilities time series for the respective sample period (see also the DJ series graphs in Figures B1–B4). We calculate the standard deviation of the series and the annualized volatility. Annualized volatility is the square rooted mean of 252 times the squared return or the realized variance. The standard deviations are always lower than the annualized volatilities. The realized variances and the GK

TABLE 3 Data description

	Sample period			r_t^2		RV_t		GK_t	
Index	**Start date**	**End date**	**Obs.**	**Avol**	***SD***	**Avol**	***SD***	**Avol**	***SD***
DJ	03/01/2000	27/09/2019	4,950	0.178	0.040	0.165	0.026	0.145	0.022
KOSPI	04/01/2000	30/09/2019	4,857	0.235	0.067	0.174	0.022	0.170	0.027
CAC	03/01/2000	30/09/2019	5,034	0.222	0.052	0.182	0.022	0.175	0.021
AORD	04/01/2000	30/09/2019	4,985	0.143	0.022	0.108	0.008	0.100	0.009
IPC	03/01/2000	30/09/2019	4,953	0.202	0.044	0.144	0.018	0.155	0.017

Abbreviation: Avol, annualized volatility.

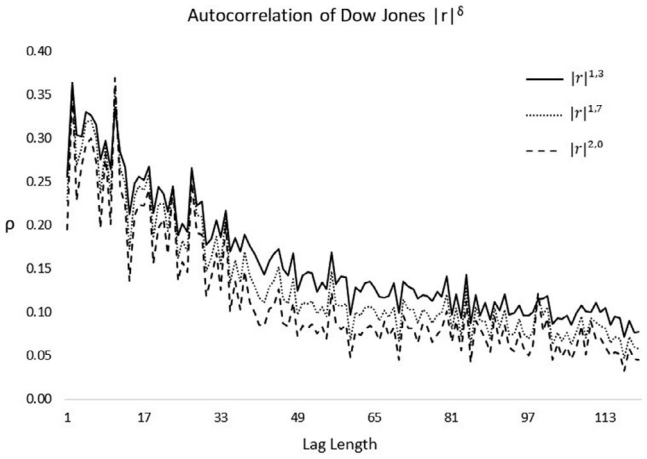

FIGURE 2 Autocorrelation of Dow Jones $|r_t|^{\delta_r}$ for $\delta_r = 1.3,1.7,$ and 2.0

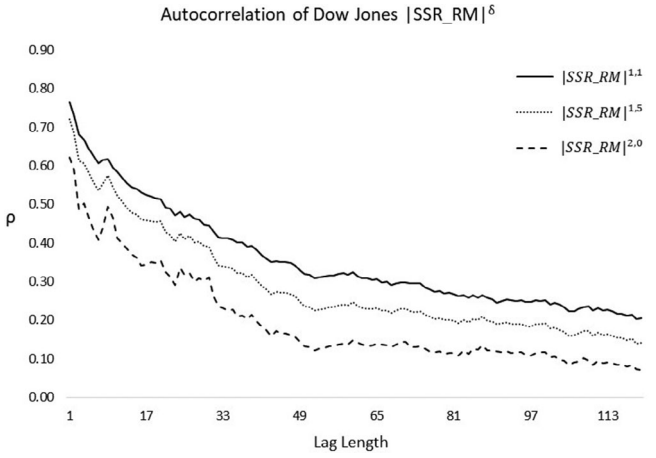

FIGURE 3 Autocorrelation of Dow Jones $|SSR\_RM_t|^{\delta_R}$ for $\delta_R = 1.1,1.5,$ and 2.0

volatilities have lower annualized volatilities and standard deviations than the squared returns since they ignore the overnight effects and are affected by less noise. The returns represent the close-to-close yield, the realized variance the open-to-close variation, and the GK volatility the open-to-close range-based variation. The annualized volatility of the realized and GK measure is between 10 and 18%, while the squared returns show figures from 14 to 24%.

Next, we examine the sample autocorrelations of the power transformed absolute returns $|r_t|^{\delta_r}$, signed square rooted realized variance $|SSR\_RM_t|^{\delta_R}$, and GK volatility $|SSR\_GK_t|^{\delta_g}$, for various values of δ_i. Figures 2, 3, and 4 show the autocorrelograms of the Dow Jones index from lag 1 to 120 for $\delta_r = 1.3,1.7,2.0$, $\delta_R = 1.1,1.5,2.0$, and $\delta_g = 1.0,1.5,2.0$ (similar autocorrelograms for the other four indices available upon request). The sample autocorrelations for $|r_t|^{1.3}$ are greater than the sample autocorrelations of $|r_t|^{\delta_r}$ for $\delta_r = 1.7,2.0$ at every lag up to at least 120 lags. In other words, the most interesting finding from the autocorrelogram is that $|r_t|^{\delta_r}$ has the strongest and slowest decaying autocorrelation when $\delta_r = 1.3$. Similarly, for the realized measure and GK volatility, the powers with the strongest autocorrelation function are $\delta_R = 1.1$ and $\delta_g = 1.0$, respectively. Furthermore, Figures 5, 6, and 7 present the sample autocorrelations of $|r_t|^{\delta_r}$, $|SSR\_RM_t|^{\delta_R}$, and $|SSR\_GK_t|^{\delta_g}$ as a function of δ_i for lags 1,12,36,72 and 96. For example, for lag 12, the highest autocorrelation values of power transformed absolute returns and signed square rooted realized and GK volatility are calculated closer to the power of 1.5 and 1.0, respectively. These figures explain our motivation to extend the benchmark HEAVY through the APARCH framework of Ding et al. (1993) and confirm the power choice of our econometric models, which is $\delta_r = 1.3$ for returns, $\delta_R = 1.1$ for the realized measure, and $\delta_g = 1.0$ for GK volatility (see Section 4).

4.2 | Estimated models

Building upon the introduction of the GARCH-X process by Engle (2002b) to include realized measures as exogenous regressors in the conditional variance equation,

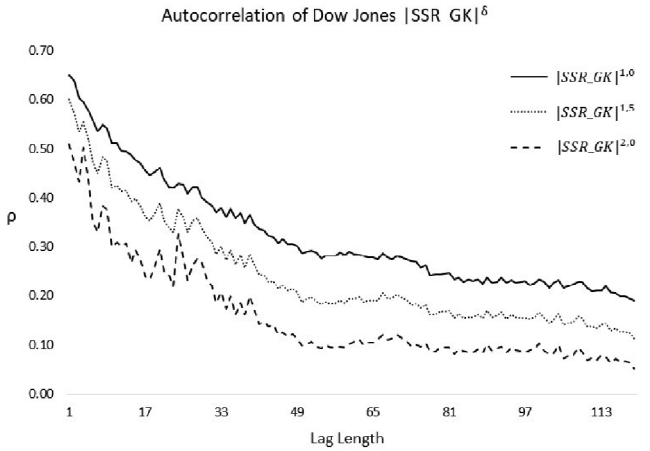

FIGURE 4 Autocorrelation of Dow Jones $|SSR\_GK_t|^{\delta_g}$ for $\delta_g = 1.0,1.5$, and 2.0

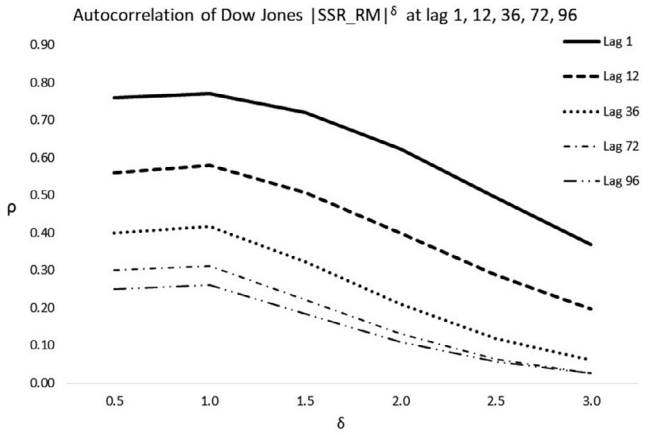

FIGURE 6 Autocorrelation of Dow Jones $|SSR\_RM_t|^{\delta_R}$ at lags 1,12,36,72, and 96

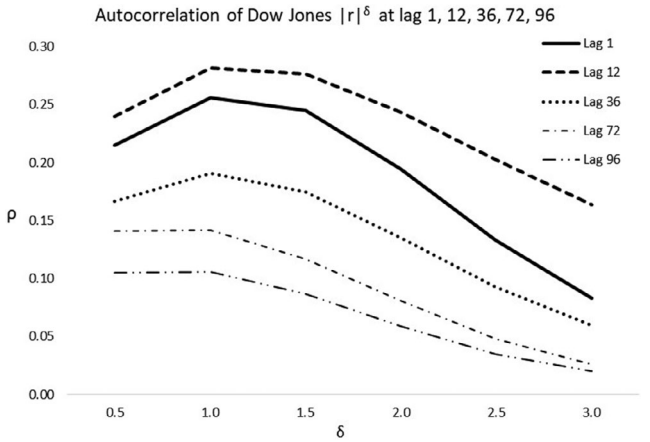

FIGURE 5 Autocorrelation of Dow Jones $|r_t|^{\delta_r}$ at lags 1,12,36,72, and 96

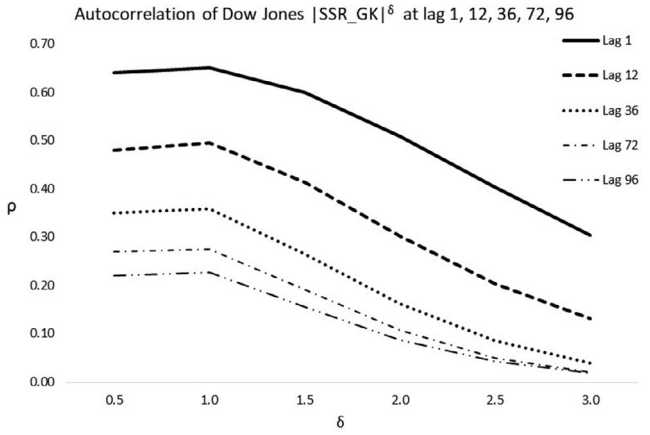

FIGURE 7 Autocorrelation of Dow Jones $|SSR\_GK_t|^{\delta_g}$ at lags 1,12,36,72, and 96

Han (2015) and Han and Kristensen (2014) studied the asymptotic properties of this new specification with a fractionally integrated (non-stationary) process included as covariate (see also Francq & Thieu, 2019). Moreover, Nakatani and Teräsvirta (2009) and Pedersen (2017) focused on the multivariate case, the so-called extended constant conditional correlation, which allows for volatility spillovers and they developed inference and testing for the QMLE parameters (see also Ling & McAleer, 2003 for the asymptotic theory of vector ARMA-GARCH processes). For the extended HEAVY models, we employ the existing Gaussian QMLE and multistep-ahead predictors applied in the APARCH framework (see, for example, He & Teräsvirta, 1999; Karanasos & Kim, 2006; Laurent, 2004, and the theoretical properties derived in Section 3). Following Pedersen and Rahbek (2019), we first test for arch effects and after rejecting the conditional homoscedasticity hypothesis we apply one-sided significance tests of the covariates added to the estimated GARCH processes.

We first estimate the bivariate benchmark formulation as in Shephard and Sheppard (2010), that is, without asymmetries and power transformations, obtaining very similar results (Table 4). For the benchmark specification, the only unconditional regressor in both equations is the first lag of the RM_t. In other words, the chosen returns equation is a GARCH(1, 0)-X process leaving out the own Arch effect, α_{rr}, from lagged squared returns since it becomes insignificant when we add the cross effect of the lagged realized measure as regressor, with a Heavy coefficient, α_{rR}, high in value and significance across all indices. The momentum parameter, β_r, is estimated around .44 to .84. For the SSR realized variance, the best-chosen model is the GARCH(1, 1) without the cross effect from lagged squared returns. The Heavy term, α_{RR}, is estimated between .25 and .47 and the

TABLE 4 The benchmark HEAVY model

	DJ	KOSPI	CAC	AORD	IPC
Panel A: Stock returns, HEAVY - r					
$(1-\beta_r L)\sigma_{rt}^2 = \omega_r + \alpha_{rR} L(RM_t)$					
β_r	.65 (15.99)***	.67 (10.58)***	.44 (7.68)***	.78 (26.61)***	.84 (28.45)***
α_{rR}	.39 (7.62)***	.62 (5.27)***	.82 (9.05)***	.37 (6.88)***	.25 (5.17)***
Q_{12}	15.43 [.22]	12.94 [.37]	12.05 [.44]	14.40 [.28]	15.40 [.21]
SBT	3.07 [.00]	2.32 [.02]	2.29 [.02]	2.60 [.01]	4.91 [.00]
lnL	−6, 336.82	−7, 599.64	−7, 762.45	−5, 728.74	−7, 582.94
Panel B: Realized measure, HEAVY − R					
$(1-\beta_R L)\sigma_{Rt}^2 = \omega_R + \alpha_{RR} L(RM_t)$					
β_R	.57 (14.06)***	.53 (13.11)***	.57 (17.08)***	.74 (30.57)***	.67 (11.56)***
α_{RR}	.44 (9.26)***	.47 (10.59)***	.42 (12.40)***	.25 (10.45)***	.33 (5.19)***
Q_{12}	12.52 [.41]	16.20 [.18]	9.54 [.66]	16.77 [.16]	16.23 [.17]
SBT	3.68 [.00]	3.49 [.00]	2.25 [.02]	2.47 [.01]	2.99 [.00]
lnL	−5, 930.41	−6, 140.66	−6, 819.26	−4, 362.39	−5, 823.11

Note: The numbers in parentheses are t-statistics. ***, **, and * denote significance at the .01, .05, and .10 level, respectively. Q_{12} is the Box-Pierce Q-statistics on the standardized residuals with 12 lags. SBT denotes the sign bias test of Engle and Ng (1993). lnL denotes the log-likelihood value for each specification. The numbers in square brackets are p-values.

momentum, β_R, is around .53 to .74. The benchmark system of equations chosen (three alternative GARCH models are tested for each dependent variable with order: (1, 1), (1, 0)-X, and the most general one, that is, (1, 1)-X) is the same as in Shephard and Sheppard (2010) with similar parameter values and the identical conclusion that the realized measure of variation does all the work of moving around the conditional variances of stock returns and the SSR realized variance. The benchmark's conclusion, as we show in this study, does not hold for the more richly parametrized asymmetric power model. More importantly, according to the SBT statistics, the asymmetric effect is obviously omitted from the benchmark specification with the sign coefficient always significant (p-values lower than .02).

Moving to our proposed extension of the benchmark bivariate system, Table 5, Panels A–C presents the estimation results for the chosen three-dimensional asymmetric power specifications (see also the 3D-benchmark model in Table C1). Wald and t-tests are used to test the significance of the Heavy, Arch, and Garman parameters, rejecting the null hypothesis at 10% in all cases. We should highlight the fact that since all the parameters take non-negative values, we use one-sided tests (see, for example, Pedersen & Rahbek, 2019).

For all three dependent variables, we statistically prefer the double asymmetric power (DAP) specification since most power transformed conditional variances are significantly affected by own and cross asymmetries. KOSPI's realized measure equation is the only case where we prefer the cross asymmetric power (CAP) model since own asymmetries are insignificant and therefore excluded. Furthermore, we estimate the power terms separately with a two-stage procedure, as follows: We, first, estimate univariate asymmetric power specifications for the returns, the realized measure, and GK volatility. The Wald tests for the estimated power terms (available upon request) reject the hypothesis of $\delta_i = 2$ in all cases. In the second stage, we use the estimated powers, δ_r, δ_R, and δ_g, from the first step to power transform each series' conditional variance and incorporate them into the trivariate model. The sequential procedure produces the fixed power term values, which are the same for the three specifications (δ_r, δ_R, and δ_g are common for Panels A, B, and C).

For the returns, the estimated power, δ_r, is between 1.30 and 1.60 (see Table 5, Panel A). The Heavy asymmetry parameter, γ_{rR}, is significant and around 0.06 (min. value) to 0.13 (max. value). Although α_{rr} is insignificant

TABLE 5 The 3D-DAP-HEAVY model

	DJ	KOSPI	CAC	AORD	IPC
Panel A: Stock returns					
$(1-\beta_r L)\left(\sigma_{rt}^2\right)^{\frac{\delta_r}{2}} = \omega_r + \gamma_{rr} s_{t-1} L\left(r_t^2\right)^{\frac{\delta_r}{2}} +$					
$\gamma_{rR} s_{t-1} L(RM_t)^{\frac{\delta_R}{2}} + \alpha_{rg} L(GK_t)^{\frac{\delta_g}{2}}$					
β_r	.81 (45.11)***	.82 (25.25)***	.80 (24.33)***	.87 (55.05)***	.91 (65.59)***
α_{rg}	.10 (4.78)***	.13 (4.66)***	.12 (3.19)***	.08 (3.83)***	.07 (3.99)***
γ_{rr}	0.08 (5.08)***	0.09 (4.84)***	0.10 (6.00)***	0.09 (6.46)***	0.11 (8.39)***
γ_{rR}	0.10 (4.76)***	0.12 (3.48)***	0.13 (4.32)***	0.07 (2.76)***	0.06 (3.90)***
δ_r	1.30	1.50	1.40	1.60	1.60
δ_R	1.10	1.20	1.10	1.30	1.00
δ_g	1.00	1.20	1.10	1.20	1.20
Q_{12}	15.89 [.20]	11.64 [.48]	15.12 [.24]	13.73 [.19]	8.12 [.62]
SBT	1.16 [.24]	0.84 [.40]	0.31 [.75]	0.41 [.68]	0.11 [.91]
lnL	−5, 974.12	−6, 933.25	−7, 078.02	−5, 584.51	−6, 890.68
Panel B: Realized measure					
$(1-\beta_R L)\left(\sigma_{Rt}^2\right)^{\frac{\delta_R}{2}} = \omega_R +$					
$(\alpha_{RR} + \gamma_{RR} s_{t-1}) L(RM_t)^{\frac{\delta_R}{2}} +$					
$\gamma_{Rr} s_{t-1} L\left(r_t^2\right)^{\frac{\delta_r}{2}} + \alpha_{Rg} L(GK_t)^{\frac{\delta_g}{2}}$					
β_R	.71 (41.14)***	.62 (25.07)***	.72 (36.11)***	.81 (47.29)***	.73 (31.23)***
α_{RR}	.10 (5.62)***	.27 (12.04)***	.16 (7.57)***	.05 (3.43)***	.19 (9.48)***
α_{Rg}	.12 (7.94)***	.06 (3.83)***	.05 (4.38)***	.08 (5.96)***	.05 (4.33)***
γ_{RR}	0.05 (5.09)***		0.03 (3.61)***	0.04 (4.60)***	0.03 (2.82)***
γ_{Rr}	0.08 (8.23)***	0.04 (9.44)***	0.05 (11.25)***	0.04 (6.75)***	0.09 (5.74)***
δ_R	1.10	1.20	1.10	1.30	1.00
δ_r	1.30	1.50	1.40	1.60	1.60
δ_g	1.00	1.20	1.10	1.20	1.20
Q_{12}	15.18 [.23]	14.40 [.28]	15.16 [.23]	13.72 [.19]	13.68 [.20]
SBT	0.64 [.52]	0.71 [.48]	0.74 [.46]	1.01 [.31]	1.12 [.26]
lnL	−5, 264.81	−5, 346.23	−5, 865.78	−4, 151.74	−5, 230.93
Panel C: GK volatility					
$\left(1-\beta_g L\right)\left(\sigma_{gt}^2\right)^{\frac{\delta_g}{2}} = \omega_g + \gamma_{gg} L(GK_t)^{\frac{\delta_g}{2}} +$					
$\alpha_{gR} s_{t-1} L(RM_t)^{\frac{\delta_R}{2}} + \gamma_{gr} s_{t-1} L\left(r_t^2\right)^{\frac{\delta_r}{2}}$					
β_g	.76 (35.34)***	.65 (18.49)***	.75 (28.51)***	.82 (44.50)***	.84 (42.41)***
α_{gR}	.11 (8.07)***	.26 (9.18)***	.16 (7.44)***	.09 (7.93)***	.09 (5.57)***
γ_{gg}	0.07 (7.87)***	0.02 (1.77)*	0.05 (5.82)***	0.03 (3.52)***	0.03 (3.11)***
γ_{gr}	0.05 (6.62)***	0.05 (7.85)***	0.04 (8.33)***	0.04 (6.83)***	0.05 (8.66)***
δ_g	1.00	1.20	1.10	1.20	1.20
δ_r	1.30	1.50	1.40	1.60	1.60
δ_R	1.10	1.20	1.10	1.30	1.00
Q_{12}	13.70 [.32]	14.98 [.24]	15.04 [.24]	13.75 [.30]	13.72 [.31]
SBT	0.78 [.44]	0.91 [.36]	1.16 [.25]	0.90 [.37]	1.08 [.28]
lnL	−4, 990.36	−5, 213.30	−5, 677.71	−3, 421.67	−5, 838.98

Note: See notes in Table 4.

and excluded in all cases, the own asymmetry parameter is significant with $\gamma_{rr} \in 0.08,0.11]$. In addition, the cross Garman parameter, α_{rg}, is significant and $.07 \leq \alpha_{rg} \leq .13$ in all cases. In other words, the lagged values of all three powered variables, that is, the negative signed realized measure, the squared negative returns, and the GK volatility, drive the model of the power transformed conditional variance of returns. Moreover, the momentum parameter, β_r, is estimated to be around .80 to .90. Obviously, all five indices generated very similar DAP specifications.

Similarly, for the realized measure the most preferred specification is the DAP one in most cases, as the estimated power is $\delta_R \in [1.00,1.30]$ (see Table 5, Panel B). Both Heavy parameters, α_{RR} and γ_{RR}, are mostly significant: α_{RR} is around .05 (min. value) to .27 (max. value), while γ_{RR}, is between 0.03 and 0.05. Only for the KOSPI index, the own asymmetries are insignificant and excluded. Moreover, the cross Arch asymmetry parameter is significant with $\gamma_{Rr} \in 0.04,0.09]$, as well as the cross Garman parameter, α_{Rg}, (with estimated values between .05 and .12). This means that the power transformed conditional variance of $\tilde{RM}_t$ is significantly affected by the lagged values of all three powered variables: squared negative returns, realized measure, and GK volatility. Lastly, the momentum parameter, β_R, is estimated to be around .62 to .81.

Finally, regarding the GK volatility the DAP specification is again the chosen one (see Table 5, Panel C). In particular, the own power term is $1.00 \leq \delta_g \leq 1.20$ in all cases. In addition, the Heavy (α_{gR}), the own asymmetry, γ_{gg}, and the Arch asymmetry, γ_{gr}, parameters are significant in all cases. In other words, the first lags of all three powered variables (realized measure, negative signed GK volatility, and squared negative returns) drive the model of the power transformed conditional variance of $\tilde{GK}_t$.

Overall, our results show strong Heavy effects (captured by the γ_{rR}, α_{RR}, γ_{RR}, and α_{gR} parameters), asymmetric Arch influences (as the estimated γ_{rr}, γ_{Rr}, and γ_{gr} are significant), as well as Garman impacts (captured by the α_{rg}, α_{Rg}, and γ_{gg} parameters). According to the log-likelihood (lnL) values reported, the log-likelihood is always higher for the DAP specifications compared to the benchmark ones, that is without asymmetries and powers, proving the superiority of our model's in-sample estimation. The SBT statistics further show that the asymmetric effect is not omitted any more since the sign coefficients are insignificant, with p-values consistently higher than .24 (see also Data S1 on the empirical application of the trivariate AP specification with long memory [Section A] and structural breaks [Section B]).

Lastly, we estimated the trivariate system of the extended HEAVY models with four alternative correlation models: the constant conditional correlations (CCC; Bollerslev, 1990), the dynamic conditional correlations (DCC; Engle, 2002a), the asymmetric dynamic conditional correlations (ADCC; Cappiello, Engle, & Sheppard, 2006) and the dynamic equicorrelations (DECO; Engle & Kelly, 2012). For simplicity, hereafter, we will assume that $\delta_i = 2$ for all $i = 1, ..., N$. The conditional covariance matrix for the N-dimensional vector $\mathbf{r}_t$, $\mathbf{H}_t$ (see Section 3.2, as well), when the conditional correlation matrix is time-varying and is denoted by $\mathbf{R}_t$, can be written as:

$$\mathbf{H}_t = \Sigma_t \mathbf{R}_t \Sigma_t,$$

where the elements occupying the off-diagonal entries of $\mathbf{R}_t$ are given by $\rho_{ij,t} = \sigma_{ij,t}/\sigma_{it}\sigma_{jt}$ for $i \neq j$. In our HEAVY model, we initially assumed that the conditional covariances and dynamic correlations are zero: $\rho_{ij,t} = \sigma_{ij,t} = 0$ for all t and $i \neq j$. This implies that $\mathbf{R}_t = \mathbf{I}$ and $\mathbf{H}_t$ is a diagonal matrix ($\mathbf{H}_t = \Sigma_t^2$). Allowing for non-zero conditional correlations does not alter our estimation results because the estimation of various non-zero correlation models: the four alternative specifications, namely the CCC, DCC, ADCC, and DECO—is a two-step procedure, where in the first step the parameters in the Σ_t matrix are estimated using the conditional variance equations, while the second step consists of estimating the (off-diagonal) parameters in $\mathbf{R}_t$ (or $\mathbf{R}$ for the CCC case). To see this more explicitly, we present the quasi-likelihood (QL) function. But first, note that $\mathbf{r}_t$ can be written as (see Equation 4):

$$\mathbf{r}_t = \mathbf{Z}_t \boldsymbol{\sigma}_t = \Sigma_t \mathbf{e}_t, \text{or equivalently} \, \mathbf{e}_t = \Sigma_t^{-1} \mathbf{r}_t.$$

Then QL is given by:

$$\begin{aligned} QL &= QL_1 + QL_2 \\ &= \underbrace{-\sum_{t=1}^{T} \left(n\log(2\pi) + 2\log|\Sigma_t| + \mathbf{r}_t' \Sigma_t^{-2} \mathbf{r}_t \right)}_{QL_1} \\ &\quad \underbrace{-\sum_{t=1}^{T} \left(\log|\Sigma_t| + \mathbf{e}_t' \mathbf{R}_t^{-1} \mathbf{e}_t + \mathbf{e}_t' \mathbf{e}_t \right)}_{QL_2}. \end{aligned}$$

Thus in the first step the parameters of the various extensions of the multivariate HEAVY process are estimated using QL_1, and in the second step we estimate the off-diagonal element in $\mathbf{R}_t$ using the standardized residuals: $\hat{\mathbf{e}}_t = \hat{\Sigma}_t^{-1} \mathbf{r}_t$ in QL_2. In all cases, the three alternative dynamic models (DCC, ADCC, and DECO) estimate the average conditional correlations for the three volatility measures around 0.75 to 0.95 similar to the CCC constant correlation values.

TABLE 6 MSE and QLIKE of m-step-ahead out-of-sample forecasts for DJ as a ratio of the benchmark model and HLN test

	MSE				QLIKE			
Specifications ↓ m-steps →	**1**	**5**	**10**	**22**	**1**	**5**	**10**	**22**
Panel A: Stock returns (HEAVY-*r*)								
Benchmark (bivariate)	1.000	1.000	1.000	1.000	1.000	1.000	1.000	1.000
3D-DAP	**0.769**	**0.791**	**0.824**	**0.872**	**0.711**	**0.747**	**0.761**	**0.833**
Panel B: Realized measure (HEAVY-*R*)								
Benchmark (bivariate)	1.000	1.000	1.000	1.000	1.000	1.000	1.000	1.000
3D-DAP	**0.784**	**0.836**	**0.845**	**0.946**	**0.721**	**0.744**	**0.780**	**0.865**
Panel C: GK volatility (HEAVY-*g*)								
Benchmark[a]	1.000	1.000	1.000	1.000	1.000	1.000	1.000	1.000
3D-DAP	**0.804**	**0.773**	**0.850**	**0.912**	**0.832**	**0.741**	**0.841**	**0.897**

Note: Bold numbers indicate minimum values across the different specifications.
Abbreviation: MSE, mean square error.
[a]The benchmark Heavy-*g* specification is defined in Table C1, Panel C (trivariate benchmark).

TABLE 7 HLN forecast encompassing test results for DJ (*p*-values)

Specifications ↓	**m-steps →**	**1**	**5**	**10**	**22**
Panel A: Stock returns (HEAVY-*r*)					
Benchmark versus 3D-DAP	.011		.019	.033	.041
Panel B: Realized measure (HEAVY-*R*)					
Benchmark versus 3D-DAP	.017		.022	.036	.053
Panel C: GK volatility (HEAVY-*g*)					
Benchmark versus 3D-DAP	.020		.015	.038	.046

Note: The numbers reported are *p*-values of the HLN (1998) test of the null hypothesis for equal forecasting performance against the one-sided alternative that the 3D-DAP outperforms the nested benchmark specification.

TABLE 8 VaR backtesting results and descriptive statistics for the DJ portfolio

	Backtesting results No. of exceptions		**Descriptive statistics**			
			99% VaR		**95% VaR**	
Specifications	**99% VaR**	**95% VaR**	**Mean**	**Min.**	**Mean**	**Min.**
Panel A: Stock returns (HEAVY-*r*)						
Benchmark (bivariate)	1	3	−700.04	−1,418.87	−494.97	−1,003.22
3D-DAP	1	3	−656.75	−1,346.29	−468.80	−951.90
Panel B: Realized measure (HEAVY-*R*)						
Benchmark (bivariate)	1	3	−632.24	−934.48	−447.03	−660.72
3D-DAP	1	3	**−641.20**	**−1,241.32**	−456.90	−877.68

Note: Mean and Min. denote the average and minimum VaR estimate, respectively. Bold numbers indicate the preferred specifications for the lower market risk capital charge with the higher loss coverage.

All in all, the conditional correlations extension does not improve further the 3D-DAP-HEAVY formulation since it provides identical results for the conditional variance equations and estimates similar correlation levels for all indices' formulations (results not reported but available upon request).

5 | FORECAST EVALUATION

Following the in-sample estimation of the proposed extensions to the HEAVY system of equations, we perform multistep-ahead out-of-sample forecasting in order to compare the forecasting accuracy of the enriched

specifications proposed in this study with the benchmark model introduced by Shephard and Sheppard (2010). We compute 1-, 5-, 10-, and 22-step-ahead forecasts of the (power transformed) conditional variances for the benchmark and the 3D-DAP models. We apply a rolling window in-sample estimation using 2,500 observations (the initial in-sample estimation period for DJ spans from 3 January 2000 until 24 December 2009). Each model is reestimated daily based on the 2,500-day rolling sample. The resulted out-of-sample forecasts of each specification calculated for DJ are as follows: 2,450 one-step-ahead, 2,446 five-step-ahead, 2,441 ten-step-ahead, and 2,439 twenty-two-step-ahead forecasted variances.

We then use the time series of the forecasted values to compute the mean square error (MSE) and the QLIKE Loss Function (Patton, 2011) of each point forecast compared to the respective actual value. For each formulation and each forecast horizon, we calculate the average MSE and QLIKE to build the ratio of the forecast losses for each extended HEAVY specification to the loss of the benchmark one. A ratio lower than the unity indicates the forecasting superiority of the proposed models relative to the benchmark one. The lowest ratio means lowest forecast losses, that is the model with the best forecasting performance. Based on the MSE calculations, we further apply the test for the pairwise comparison of nested models (here the benchmark specification vs. the AP extensions) suggested by Harvey, Leybourne, and Newbold (1998), HLN thereafter. The HLN forecast encompassing test was introduced as a modification to the Diebold–Mariano test (Diebold & Mariano, 1995) to account for the fact that models are nested (here the 3D-DAP nests the benchmark specification). HLN test whether the differences between the two competing formulations' forecasts are statistically significant and the larger model's forecast losses are lower than the nested model's ones (see also Clark & McCracken, 2001).

We apply the optimal predictor $|\mathbf{r}_t|^{\wedge\boldsymbol{\delta}}$ (under Proposition 3 in Section 3.2.3) and calculate the out-of-sample forecasts. The results, presented in Tables 6 and 7 for the DJ index (similar forecasting results for the other four indices available upon request), clearly show the preference for our extensions over the benchmark models across all time horizons. The 3D-DAP specification dominates the benchmark model with the lowest MSE and QLIKE (Table 6). Given the HLN test, the asymmetric power formulation performs significantly better than the benchmark HEAVY model in the short- and long-term horizons, with the computed forecasts significantly closer to the actual values for the enriched HEAVY formulations. HLN test results reject the null hypothesis of equal forecasts in favour of the 3D-DAP model's lower forecast losses at 5% significance level (Table 7). Investors, traders and risk managers can benefit from the superior short-term forecasts for 1–10 days, while policymakers should focus on the longer-term forecasting performance to predict 'safely' the 1-month-forward financial volatility given the significant range-based effects.

The forecasting performance of the proposed models can be further examined in a real-world risk management empirical example. VaR is a daily metric for market risk measurement, defined as the potential loss in the value of a portfolio, over a pre-defined holding period, for a given confidence level. The most important input in the VaR calculation is the 1-day volatility forecast of the risk factor relevant to the trading portfolio under scope. We directly apply our conditional variance forecasts in a long portfolio position to one Dow Jones industrial average index contract starting from 7 May 2019. We calculate 100 daily VaR values from 8 May 2019 to 27 September 2019 using the 1-day conditional variance forecasts of each model for returns and realized measure (four models in total). Given that the conditional mean return is zero and the returns follow the normal distribution, we, first, calculate the 1-day VaR with 99 and 95% confidence level. According to the parametric approach to VaR calculation, we multiply the daily portfolio value with the 1-day-ahead conditional volatility forecast (equal to the square root of the conditional variance forecast) and the left quantile at the respective confidence level of the normal distribution (the z-scores for 99 and 95% confidence level are 2.326 and 1.645, respectively). Secondly, we calculate the daily realized return of the portfolio (gains and losses) and, thirdly, we perform the backtesting exercise, comparing the realized returns with the respective 1-day VaR for the 99 and 95% confidence levels. In the cases where the realized loss exceeds the respective day's VaR value, we record it as an exception in the backtesting procedure, meaning that the VaR metric fails to cover the loss of the specific day's portfolio value.

According to the backtesting results (see Table 8: Backtesting results, No. of Exceptions), the number of exceptions across all models is in line with the selected confidence level (the 99 and 95% confidence levels allow for 1 and 5 exceptions, respectively, every 100 days) and low enough to prevent supervisors from increasing the capital charges (in which case we refer to a bank's trading portfolio). The higher number of exceptions means higher market risk capital requirements for financial institutions since regulators heavily penalize banks' internal models that fail to cover trading losses through the VaR estimates. Following the Basel traffic light approach, the market risk capital charge increases when the backtesting exceptions are more than 4 in a sample of 250 daily observations and 99% confidence level. Since all

models provide adequate coverage of the realized losses, we should further compare the average and minimum VaR estimates calculated based on the forecasts of each specification (Table 8: Descriptive statistics). The VaR estimate that provides the higher loss coverage with the lower capital charges is the one with the lower minimum and higher mean values. This is achieved by the realized measure specifications, where we prefer the asymmetric power model, augmented with the range-based volatility impact. Given that the market risk capital requirement is calculated on the trading portfolio total 99% VaR (absolute value, 60-day average) adjusted by the penalty of the backtesting exceptions (higher than 4 in the 250-day sample), the bank needs the smallest possible VaR average with the larger minimum estimate in absolute terms. Thereupon, our proposed models clearly satisfy both criteria, contributing to the risk manager's VaR calculation of the volatility forecasts that better capture the loss distribution (higher extreme loss coverage with higher absolute minimum value) without inflating the capital charges (lower absolute mean).

Furthermore, the volatility forecasts produced by the 3D-DAP-HEAVY model are directly applicable to a wide range of business finance operations, alongside the well-established risk management practice outlined in the VaR empirical exercise. Portfolio managers should rely on the proposed framework to predict future volatility in asset allocation and minimum-variance portfolio selection complying with their clients' risk appetite. Risk-averse investors' mandates specify low volatility boundaries on their portfolio positions, while risk lovers allow for higher volatilities on the risk–return trade-off of their investments. Accurate volatility predictions can also be used in a forward-looking performance evaluation context, through the risk-adjusted metrics, that is, the Sharpe or the Treynor risk-adjusted return ratios. Traders and risk managers focus on the volatility trajectory in derivatives pricing, volatility targeting strategies, and several other trading decisions. Trading and hedging in financial markets depend on risk factors whose predicted volatilities are the main input of any pricing function applied. Moreover, financial chiefs consider volatility forecasts when they decide on investment projects or funding choices (bond and equity valuation defining the cost of capital) given that expected future cash-flow variation is a critical factor in business analytics.

Finally, policymakers and authorities supervising and regulating the financial system should take into account reliable volatility forecasts in designing macro- and micro-prudential policy responses. The risk management of the financial system is structured as follows: (i) identification of risk sources (both endogenous—financial market volatility—and exogenous—the macroeconomy), (ii) assessment of the nature of risk factors, (iii) risk measurement (micro-prudential metrics at the financial institution level and macro-prudential metrics at the system and markets level), and (iv) risk mitigation with proactive regulation and crisis preparedness plans and strategies. Therefore, regulators should employ the range-informed financial volatility forecasts of the 3D-DAP-HEAVY model across the whole risk management process and the financial stability oversight tools, such as the early warning systems, the macro stress-tests on financial institutions and the bank capital and risk frameworks. For example, the macro stress-test scenario inputs, which include, among others, stock market volatility predictions for the financial institutions' trading books, should consider range-informed volatility estimates. Furthermore, complying with the capital and risk frameworks set by supervisors (Basel committee and central banks), financial institutions measure their trading portfolio's market risk (beyond the credit risk of their loan portfolio) with the daily VaR metric. Given that reliable volatility forecasts, provided by our superior modelling framework, improve the VaR estimates considerably, supervisors should encourage banks to improve their market risk internal models with more accurate range-informed volatility forecasts based on both low- and high-frequency data.

6 | CONCLUSIONS

Our study has extended the bivariate HEAVY system to the three-dimensional DAP specification. Our major contribution to volatility modelling research within this HEAVY framework is twofold: We, firstly, augment the benchmark model with a third variable, that is the range-based volatility, in order to achieve greater accuracy in volatility forecasting. Secondly, we enrich the trivariate formulation by taking into consideration leverage and power characteristics. Thirdly, we derive the theoretical time series properties (optimal predictors and second moment structure) of the multivariate asymmetric power system and assess its finite-sample performance through a simulation study. Our empirical results favour the most general asymmetric power specification, where the lags of all three powered variables—squared negative returns, GK volatility, and realized variance—move the dynamics of each power transformed conditional variance. The asymmetric response to negative and positive shocks and its power transformations ensure the superiority of our contribution, which can be implemented on the areas of asset allocation and portfolio selection, as well as on several risk management practices. Further, we provide evidence on the forecasting superiority of our extensions

over the benchmark HEAVY model through the rolling window out-of-sample forecasting across multiple short- and long-term horizons.

Our empirical findings on the nexus between low-frequency daily squared returns, range-based volatility, and high-frequency intra-daily realized measures, provide a volatility forecasting framework with important implications for policymakers and market practitioners, from investors, risk and portfolio managers up to financial chiefs, leaving ample room for future research on further model extensions. Thereupon, policymakers and market players should use our HEAVY framework to closely watch and forecast financial volatility patterns in the process of devising drastic policies, enforcing the financial system's regulations to preserve financial stability, deciding on asset allocation, hedging strategies, and investment projects. As part of future research, it would be interesting to extend the theoretical framework of the asymmetric power system with long memory features and structural breaks (supporting our empirical illustrations in Data S1). A further interesting line of future research could be the enrichment of the multivariate HEAVY formulation of Noureldin, Shephard, and Sheppard (2012) with leverage, power transformations, and long memory, extending the recent study of Dark (2018), who has applied a long memory multivariate GARCH model to the multivariate HEAVY, or Opschoor, Janus, Lucas, and Van Dijk (2018) within the generalized autoregressive score (GAS) process of Creal, Koopman, and Lucas (2013).

DATA AVAILABILITY STATEMENT

The data that support the findings of this study are publicly available in the Oxford-Man Institute Realized Library at https://realized.oxford-man.ox.ac.uk/data/download.

ORCID

Stavroula Yfanti https://orcid.org/0000-0001-8071-916X
Menelaos Karanasos https://orcid.org/0000-0001-5442-3509

ENDNOTES

[1] The acronym HEAVY is derived by 'High-frEquency-bAsed VolatilitY' in Shephard and Sheppard (2010).

[2] This type of asymmetry was introduced by Glosten, Jagannathan, and Runkle (1993).

[3] The benchmark HEAVY specification as established by Shephard and Sheppard (2010) does not incorporate our third variable, that is GK volatility.

REFERENCES

Andersen, T. G., & Bollerslev, T. (1998). Answering the skeptics: Yes, standard volatility models do provide accurate forecasts. *International Economic Review*, *39*, 885–905.

Andersen, T. G., Bollerslev, T., Diebold, F. X., & Labys, P. (2001). The distribution of exchange rate volatility. *Journal of the American Statistical Association*, *96*, 42–55.

Barndorff-Nielsen, O. E., Hansen, P. R., Lunde, A., & Shephard, N. (2008). Designing realized kernels to measure the ex-post variation of equity prices in the presence of noise. *Econometrica*, *76*, 1481–1536.

Barndorff-Nielsen, O. E., Hansen, P. R., Lunde, A., & Shephard, N. (2009). Realized kernels in practice: Trades and quotes. *The Econometrics Journal*, *12*, C1–C32.

Barndorff-Nielsen, O. E., & Shephard, N. (2002). Econometric analysis of realized volatility and its use in estimating stochastic volatility models. *Journal of the Royal Statistical Society, Series B*, *64*, 253–280.

Bollerslev, T. (1986). Generalized autoregressive conditional heteroskedasticity. *Journal of Econometrics*, *31*, 307–327.

Bollerslev, T. (1990). Modelling the coherence in short-run nominal exchange rates: A multivariate generalized ARCH model. *Review of Economics and Statistics*, *72*, 498–505.

Borovkova, S., & Mahakena, D. (2015). News, volatility and jumps: The case of natural gas futures. *Quantitative Finance*, *15*, 1217–1242.

Brooks, R. D., Faff, R. W., McKenzie, M. D., & Mitchell, H. (2000). A multi-country study of power ARCH models and national stock market returns. *Journal of International Money and Finance*, *19*, 377–397.

Cappiello, L., Engle, R. F., & Sheppard, K. (2006). Asymmetric dynamics in the correlations of global equity and bond returns. *Journal of Financial Econometrics*, *4*, 537–572.

Chen, Z., Daigler, R., & Parhizgari, A. (2006). Persistence of volatility in future markets. *Journal of Futures Markets*, *26*, 571–594.

Chou, R. Y., Chou, H., & Liu, N. (2010). Range volatility models and their applications in finance. In C.-F. Lee & J. Lee (Eds.), *Handbook of quantitative finance and risk management* (pp. 1273–1282). New York, NY: Springer.

Chou, R. Y., Chou, H., & Liu, N. (2015). Range volatility: A review of models and empirical studies. In C.-F. Lee & J. Lee (Eds.), *Handbook of financial econometrics and statistics* (pp. 2029–2050). New York, NY: Springer.

Clark, T. E., & McCracken, M. W. (2001). Tests for equal forecast accuracy and encompassing for nested models. *Journal of Econometrics*, *105*, 85–110.

Conrad, C., & Karanasos, M. (2010). Negative volatility spillovers in the unrestricted ECCC-GARCH model. *Econometric Theory*, *26*, 838–862.

Corsi, F., Mittnik, S., Pigorsch, C., & Pigorsch, U. (2008). The volatility of realized volatility. *Econometric Reviews*, *27*, 46–78.

Creal, D. D., Koopman, S. J., & Lucas, A. (2013). Generalized autoregressive score models with applications. *Journal of Applied Econometrics*, *28*, 777–795.

Dark, J. G. (2018). Multivariate models with long memory dependence in conditional correlation and volatility. *Journal of Empirical Finance*, *48*, 162–180.

Diebold, F. X., & Mariano, R. S. (1995). Comparing predictive accuracy. *Journal of Business and Economic Statistics*, *13*, 253–263.

Ding, Z., Granger, C. W. J., & Engle, R. F. (1993). A long memory property of stock market returns and a new model. *Journal of Empirical Finance*, *1*, 83–106.

Engle, R. F. (2002a). Dynamic conditional correlation: A simple class of multivariate generalized autoregressive conditional heteroskedasticity models. *Journal of Business and Economic Statistics*, *20*, 339–350.

Engle, R. F. (2002b). New frontiers for ARCH models. *Journal of Applied Econometrics*, *17*, 425–446.

Engle, R. F., & Kelly, B. T. (2012). Dynamic equicorrelation. *Journal of Business and Economic Statistics*, *30*, 212–228.

Engle, R. F., & Ng, V. K. (1993). Measuring and testing the impact of news on volatility. *The Journal of Finance*, *48*, 1749–1778.

Francq, C., & Thieu, L. Q. (2019). QML inference for volatility models with covariates. *Econometric Theory*, *35*, 37–72.

Garman, M., & Klass, M. (1980). On the estimation of security price volatilities from historical data. *Journal of Business*, *53*, 67–78.

Glosten, L. R., Jagannathan, R., & Runkle, D. E. (1993). On the relation between the expected value and the volatility of the nominal excess return on stocks. *The Journal of Finance*, *48*, 1779–1801.

Halunga, A. G., & Orme, C. D. (2009). First-order asymptotic theory for parametric misspecification tests of GARCH models. *Econometric Theory*, *25*, 364–410.

Han, H. (2015). Asymptotic properties of GARCH-X processes. *Journal of Financial Econometrics*, *13*, 188–221.

Han, H., & Kristensen, D. (2014). Asymptotic theory for the QMLE in GARCH-X models with stationary and nonstationary covariates. *Journal of Business & Economic Statistics*, *32*, 416–429.

Hansen, P. R., Huang, Z., & Shek, H. (2012). Realized GARCH: A joint model for returns and realized measures of volatility. *Journal of Applied Econometrics*, *27*, 877–906.

Harvey, D. I., Leybourne, S. J., & Newbold, P. (1998). Tests for forecast encompassing. *Journal of Business and Economic Statistics*, *16*, 254–259.

He, C., & Teräsvirta, T. (1999). Statistical properties of the asymmetric power ARCH model. In R. F. Engle & H. White (Eds.), *Cointegration, causality, and forecasting. Festschrift in honour of Clive W.J. Granger* (pp. 462–474). Oxford, England: Oxford University Press.

Heber, G., Lunde, A., Shephard, N., & Sheppard, K. (2009). *Oxford-Man Institute's (OMI's) realized library, Version 0.2*, Oxford: Oxford-Man Institute, University of Oxford.

Huang, Z., Liu, H., & Wang, T. (2016). Modeling long memory volatility using realized measures of volatility: A realized HAR GARCH model. *Economic Modelling*, *52*, 812–821.

Karanasos, M., & Kim, J. (2006). A re-examination of the asymmetric power ARCH model. *Journal of Empirical Finance*, *13*, 113–128.

Laurent, S. (2004). Analytical derivates of the APARCH model. *Computational Economics*, *24*, 51–57.

Li, Y. N., Zhang, Y., & Zhang, C. (2019). Statistical inference for measurement equation selection in the log-RealGARCH model. *Econometric Theory*, *35*, 943–977.

Ling, S., & McAleer, M. (2003). Asymptotic theory for a vector ARMA-GARCH model. *Econometric Theory*, *19*, 280–310.

Lundbergh, S., & Teräsvirta, T. (2002). Evaluating GARCH models. *Journal of Econometrics*, *110*, 417–435.

Lütkepohl, H. (1996). *Handbook of matrices* (Vol. 1). Chichester, England: Wiley.

Molnár, P. (2012). Properties of range-based volatility estimators. *International Review of Financial Analysis*, *23*, 20–29.

Molnár, P. (2016). High–low range in GARCH models of stock return volatility. *Applied Economics*, *48*, 4977–4991.

Nakatani, T., & Teräsvirta, T. (2009). Testing for volatility interactions in the constant conditional correlation GARCH model. *The Econometrics Journal*, *12*, 147–163.

Noureldin, D., Shephard, N., & Sheppard, K. (2012). Multivariate high-frequency-based volatility (HEAVY) models. *Journal of Applied Econometrics*, *27*, 907–933.

Opschoor, A., Janus, P., Lucas, A., & Van Dijk, D. (2018). New HEAVY models for fat-tailed realized covariances and returns. *Journal of Business and Economic Statistics*, *36*, 643–657.

Patton, A. J. (2011). Volatility forecast comparison using imperfect volatility proxies. *Journal of Econometrics*, *160*, 246–256.

Pedersen, R. S. (2017). Inference and testing on the boundary in extended constant conditional correlation GARCH models. *Journal of Econometrics*, *196*, 23–36.

Pedersen, R. S., & Rahbek, A. (2019). Testing GARCH-X type models. *Econometric Theory*, *35*, 1012–1047.

Shephard, N., & Sheppard, K. (2010). Realising the future: Forecasting with high-frequency-based volatility (HEAVY) models. *Journal of Applied Econometrics*, *25*, 197–231.

SUPPORTING INFORMATION

Additional supporting information may be found online in the Supporting Information section at the end of this article.

How to cite this article: Yfanti S, Chortareas G, Karanasos M, Noikokyris E. A three-dimensional asymmetric power HEAVY model. *Int J Fin Econ*. 2022;27:2737–2761. https://doi.org/10.1002/ijfe.2296

APPENDIX A.

Second moments (Proofs)

In this section, we will derive the proofs of Theorems 2 and 3. But first we present the following lemma that we will use in the proofs below.

Lemma 1 *The* $vec\left[\mathbb{E}\left(\mathbf{A}_{t-1}\mathbf{v}_{t-1}\mathbf{v}_{t-1}'\mathbf{A}_{t-1}'\right)\right]$ *is given by*:

$$vec\left[\mathbb{E}\left(\mathbf{A}_{t-1}\mathbf{v}_{t-1}\mathbf{v}_{t-1}'\mathbf{A}_{t-1}'\right)\right] l = \quad \bar{\mathbf{A}}^{\otimes 2}\tilde{\mathbf{Z}}\left[\gamma(0)+\boldsymbol{\sigma}^{\otimes 2}\right]. \quad \text{(A1)}$$

Proof Using the definition of $\mathbf{v}_{t-1}$ in Definition 1(ii) and interchanging the vec and expectation operators, the left-hand side of Equation (A1) takes the form:

$$\mathbb{E}\left\{vec\left[\mathbf{A}_{t-1}\left(|\mathbf{Z}_t|^{\wedge\delta}-\mathbf{Z}\right)\boldsymbol{\sigma}_t^{\wedge\delta}\left(\boldsymbol{\sigma}_t^{\wedge\delta}\right)'\left(|\mathbf{Z}_t|^{\wedge\delta}-\mathbf{Z}\right)'\mathbf{A}_{t-1}'\right]\right\}.$$

Using the rules of the vec operator (see, for example, Lütkepohl, 1996, sect. 7.2) and, under Condition 2, applying the expectation operator, in view of Equation (13) the above expression yields:

$$vec\left[\mathbb{E}\left(\mathbf{A}_{t-1}\mathbf{v}_{t-1}\mathbf{v}_{t-1}'\mathbf{A}_{t-1}'\right)\right] = \mathbb{E}\left(\mathbf{A}_{t-1}^{\otimes 2}\right)\mathbb{E}\left(|\mathbf{Z}_t|^{\wedge\delta}-\mathbf{Z}\right)^{\otimes 2}\left(\boldsymbol{\gamma}(0)+\boldsymbol{\sigma}^{\otimes 2}\right). \tag{A2}$$

Since $\mathbb{E}\left(\mathbf{A}_t^{\otimes 2}\right)=\bar{\mathbf{A}}^{\otimes 2}$ and in view of Notation 8, it follows that the right-hand side of Equation (A2) equals the right-hand side of Equation (A1) as required.

Proof (of Theorem 2) Rewrite the weak VARMA representation, Equation (6), as:

$$\boldsymbol{\sigma}_t^{\wedge\delta}=\boldsymbol{\omega}+\mathbf{C}_{t-1}\boldsymbol{\sigma}_{t-1}^{\wedge\delta}+\mathbf{A}_{t-1}\mathbf{v}_{t-1}.$$

Using $\boldsymbol{\omega}=(\mathbf{I}-\mathbf{C})\boldsymbol{\sigma}$ (see Equation (11)) the above equation can be expressed in terms of deviations from the mean:

$$\boldsymbol{\sigma}_t^{\wedge\delta}-\boldsymbol{\sigma}=(\mathbf{C_{t-1}}-\mathbf{C})\boldsymbol{\sigma}+\mathbf{C}_{t-1}\left(\boldsymbol{\sigma}_{t-1}^{\wedge\delta}-\boldsymbol{\sigma}\right)+\mathbf{A}_{t-1}\mathbf{v}_{t-1}. \tag{A3}$$

Taking the transpose on both sides of Equation (A3) yields:

$$\left(\boldsymbol{\sigma}_t^{\wedge\delta}-\boldsymbol{\sigma}\right)'=\boldsymbol{\sigma}(\mathbf{C_{t-1}}-\mathbf{C})'+\left(\boldsymbol{\sigma}_{t-1}^{\wedge\delta}-\boldsymbol{\sigma}\right)'\mathbf{C}'_{t-1}+\mathbf{v}_{t-1}'\mathbf{A}_{t-1}'. \tag{A4}$$

Right-multiplying Equation (A3) by Equation (A4) and, under Condition 2, taking expectations on both sides, yields (in view of Equation (13) and ignoring zero terms):

$$\Gamma(0)=\mathbb{E}\left[\mathbf{C}_{t-1}\left(\boldsymbol{\sigma}_{t-1}^{\wedge\delta}-\boldsymbol{\sigma}\right)\left(\boldsymbol{\sigma}_{t-1}^{\wedge\delta}-\boldsymbol{\sigma}\right)'\mathbf{C}'_{t-1}\right]+\mathbb{E}\left(\mathbf{A}_{t-1}\mathbf{v}_{t-1}\mathbf{v}_{t-1}'\mathbf{A}_{t-1}'\right). \tag{A5}$$

Applying the vec operator to both sides of Equation (A5) yields:

$$\boldsymbol{\gamma}(0)=\mathbb{E}\left(\mathbf{C}_t^{\otimes 2}\right)\boldsymbol{\gamma}(0)+vec\left[\mathbb{E}\left(\mathbf{A}_{t-1}\mathbf{v}_{t-1}\mathbf{v}_{t-1}'\mathbf{A}_{t-1}'\right)\right].$$

In view of Lemma 1 and the fact that $\mathbb{E}\left(\mathbf{C}_t^{\otimes 2}\right)=\mathbf{C}^{\otimes 2}$, we have:

$$\boldsymbol{\gamma}(0)=\mathbf{C}^{\otimes 2}\boldsymbol{\gamma}(0)+\bar{\mathbf{A}}^{\otimes 2}\tilde{\mathbf{Z}}\left[\boldsymbol{\gamma}(0)+\boldsymbol{\sigma}^{\otimes 2}\right].$$

Solving the above equation for $\boldsymbol{\gamma}(0)$ gives:

$$\boldsymbol{\gamma}(0)=\left(\mathbf{I}_{N^2}-\tilde{\mathbf{C}}\right)^{-1}\bar{\mathbf{A}}^{\otimes 2}\tilde{\mathbf{Z}}\boldsymbol{\sigma}^{\otimes 2}$$

($\tilde{\mathbf{C}}$ is given in Equation (15)), which completes the proof of Equation (16).

Next, rewrite the general solution in Equation (8) as:

$$\left(\boldsymbol{\sigma}_t^{\wedge\delta}\right)'=\sum_{r=1}^{\ell}\left(\boldsymbol{\omega}'+\mathbf{v}_{t-r}'\mathbf{A}_{t-r}'\right)\mathbf{D}_{t,r-1}'+\left(\boldsymbol{\sigma}_{\mathbf{t}-\ell}^{\wedge\delta}\right)'\mathbf{D}'_{t,\ell}.$$

Left-multiplying the above equation by $\boldsymbol{\sigma}_{t-\ell}^{\wedge\delta}$, taking expectations on both sides under Condition 2, and using $\mathbb{E}(\mathbf{D}_{t,\ell})=\mathbf{C}^{\ell}$, see the text next to Equation (9), yields (in view of Equation (13) and ignoring zero terms):

$$\Sigma(\ell)=\boldsymbol{\sigma}\boldsymbol{\omega}'\left[(\mathbf{I}-\mathbf{C})^{-1}\right]'\left(\mathbf{I}-\mathbf{C}^{\ell}\right)'+\Sigma(0)\left(\mathbf{C}^{\ell}\right)'.$$

On account of $\boldsymbol{\omega}=(\mathbf{I}-\mathbf{C})\boldsymbol{\sigma}$, it follows that:

$$\Gamma(\ell)=\Gamma(0)\left(\mathbf{C}^{\ell}\right)'.$$

Applying the vec operator to both side of the above equation yields Equation (17) as claimed.

Proof (of Theorem 3) Rewrite $|\mathbf{r}_t|^{\wedge\delta}$ in terms of deviations from the mean (see Equations (4) and (12)):

$$|\mathbf{r}_t|^{\wedge\delta}-\mathbf{r}=|\mathbf{Z}_t|^{\wedge\delta}\left(\boldsymbol{\sigma}_t^{\wedge\delta}-\boldsymbol{\sigma}\right)+\left(|\mathbf{Z}_t|^{\wedge\delta}-\mathbf{Z}\right)\boldsymbol{\sigma}\text{ or}$$
$$\left(|\mathbf{r}_t|^{\wedge\delta}-\mathbf{r}\right)'=\left(\boldsymbol{\sigma}_t^{\wedge\delta}-\boldsymbol{\sigma}\right)'\left(|\mathbf{Z}_t|^{\wedge\delta}\right)'+\boldsymbol{\sigma}'\left(|\mathbf{Z}_t|^{\wedge\delta}-\mathbf{Z}\right)'.$$

Multiplying $|\mathbf{r}_t|^{\wedge\delta}-\mathbf{r}$ by its transpose, using the above expressions, taking expectations on both sides, and ignoring zero terms, it follows that the vectorization of $\Gamma_r(0)$ is given by:

$$\boldsymbol{\gamma}_r(0)=\mathbb{E}\left[\left(|\mathbf{Z}_t|^{\wedge\delta}\right)^{\otimes 2}\right]\boldsymbol{\gamma}(0)+\tilde{\mathbf{Z}}\boldsymbol{\sigma}^{\otimes 2}.$$

Applying Equation (16) to the above expression of $\boldsymbol{\gamma}_r(0)$, Equation (18) follows (the proof of Equation (19) is similar to the proof of Equation (18) and, thus it is omitted) and the proof is complete.

APPENDIX B.

Dow Jones graphs

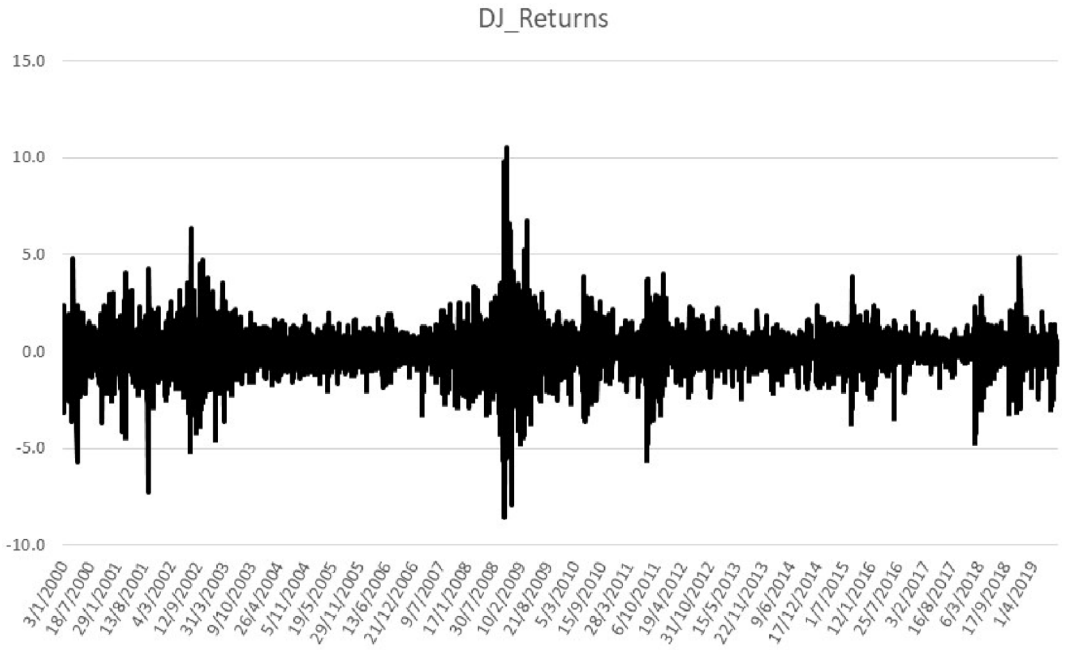

FIGURE B1 Dow Jones close-to-close returns

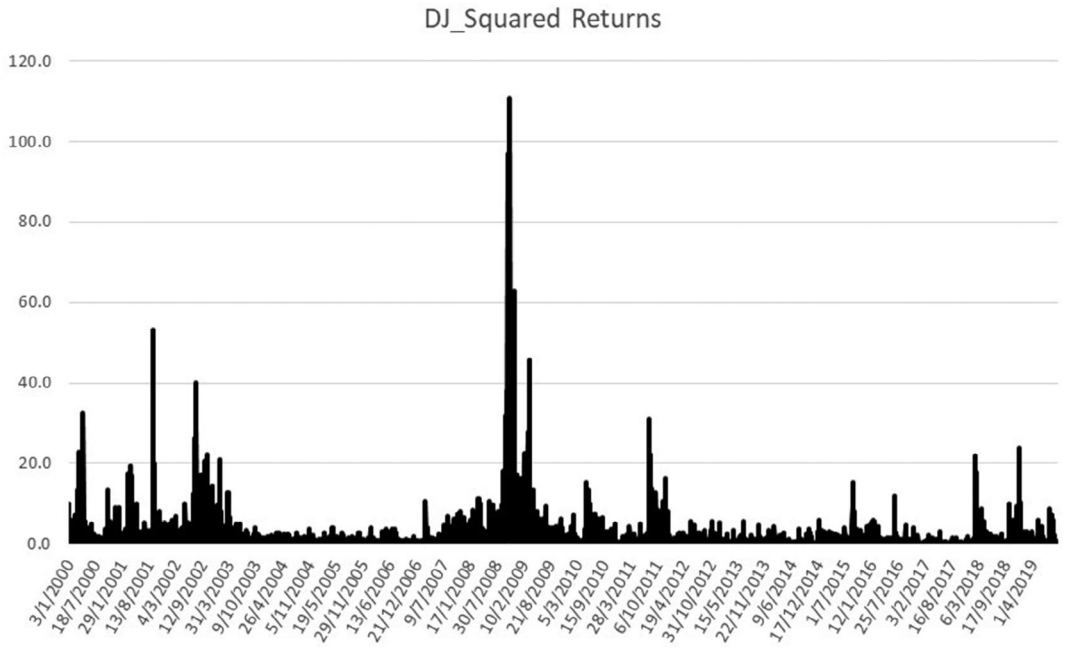

FIGURE B2 Dow Jones squared returns

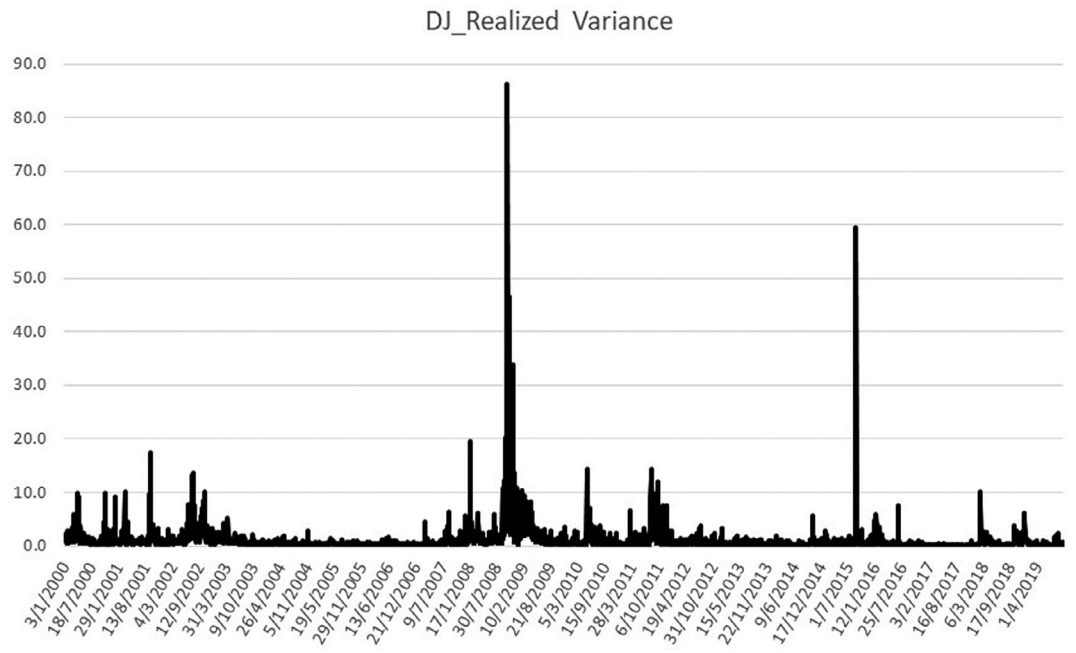

FIGURE B3 Dow Jones realized variance

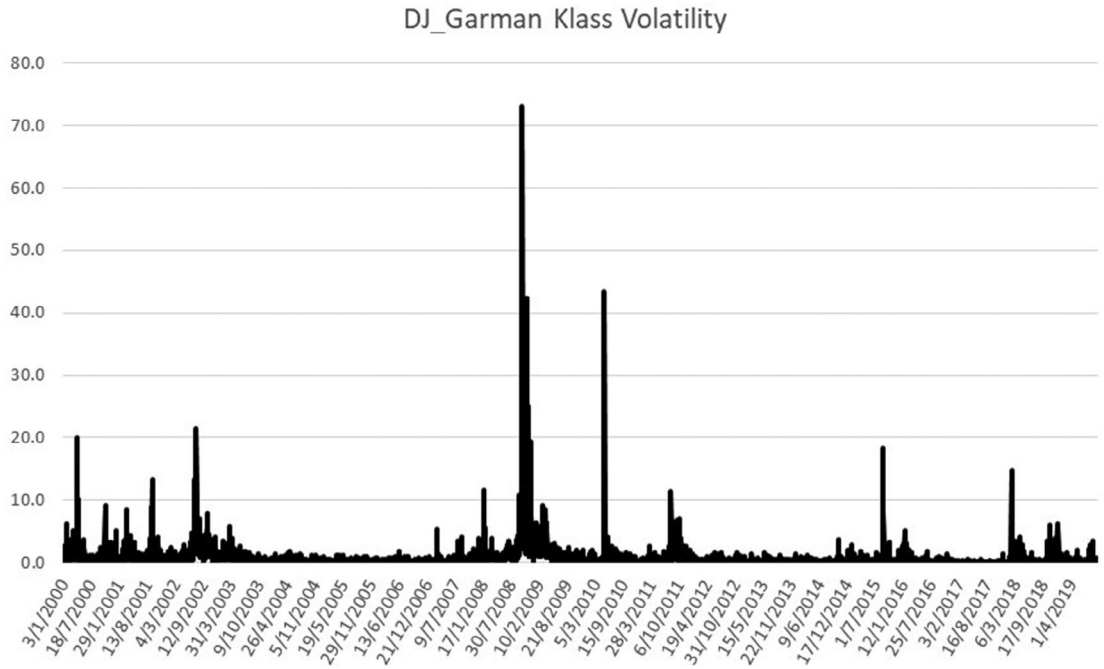

FIGURE B4 Dow Jones Garman–Klass volatility

APPENDIX C.

3D-benchmark model results

TABLE C1 The 3D-benchmark HEAVY model

	DJ	KOSPI	CAC	AORD	IPC
Panel A: Stock returns, HEAVY - r					
$(1-\beta_r L)\sigma_{rt}^2 = \omega_r + \alpha_{rR} L(RM_t) + \alpha_{rg} L(GK_t)$					
β_r	.68 (17.59)***	.67 (10.81)***	.44 (7.65)***	.77 (25.67)***	.91 (61.24)***
α_{rR}	.18 (3.36)***	.40 (2.99)***	.76 (6.66)***	.28 (4.48)***	.07 (6.78)***
α_{rg}	.23 (4.41)***	.23 (1.86)*	.06 (3.52)***	.13 (2.26)**	.20 (7.21)***
Q_{12}	16.89 [.15]	11.83 [.46]	12.19 [.43]	15.27 [.23]	16.90 [.15]
SBT	3.13 [.00]	2.53 [.01]	2.35 [.02]	2.59 [.01]	4.60 [.00]
lnL	−6, 315.85	−7, 579.14	−7, 757.28	−5, 721.07	−7, 398.91
Panel B: Realized measure, HEAVY - R					
$(1-\beta_R L)\sigma_{Rt}^2 = \omega_R + \alpha_{RR} L(RM_t) + \alpha_{Rg} L(GK_t)$					
β_R	.58 (12.42)***	.55 (13.81)***	.57 (16.89)***	.73 (28.21)***	.67 (11.04)***
α_{RR}	.31 (4.44)***	.34 (8.33)***	.36 (9.78)***	.19 (7.20)***	.26 (3.49)***
α_{Rg}	.14 (4.18)***	.11 (3.95)***	.06 (2.88)***	.09 (3.82)***	.06 (2.66)***
Q_{12}	12.85 [.38]	15.44 [.22]	9.46 [.66]	16.89 [.15]	9.53 [.48]
SBT	3.45 [.00]	5.26 [.00]	2.39 [.02]	2.67 [.01]	3.12 [.00]
lnL	−5, 922.35	−6, 135.93	−6, 818.17	−4, 357.03	−5, 816.53
Panel C: GK volatility, HEAVY - g					
$\left(1-\beta_g L\right)\sigma_{gt}^2 = \omega_g + \alpha_{gR} L(RM_t)$					
β_g	.58 (12.13)***	.50 (7.36)***	.57 (13.46)***	.75 (31.27)***	.76 (14.33)***
α_{gR}	.33 (7.67)***	.46 (7.04)***	.38 (9.84)***	.20 (9.86)***	.24 (4.44)***
Q_{12}	9.65 [.65]	12.72 [.24]	9.33 [.67]	12.39 [.26]	9.62 [.66]
SBT	4.42 [.00]	3.01 [.00]	2.85 [.00]	3.22 [.00]	8.70 [.00]
lnL	−5, 402.41	−6, 068.15	−6, 630.57	−3, 997.18	−6, 290.51

Note: See notes in Table 4.